

Naval Research Laboratory

Washington, DC 20375-5320 NRL/PU/6110--00-423



Electromagnetic Induction and Magnetic Sensor Fusion for Enhanced UXO Target Classification

Naval Research Laboratory, Washington, DC

H. H. Nelson

Chemical Dynamics and Diagnostics Branch

Chemistry Division

Bruce Barrow

AETC, Inc.



Report Documentation Page			Form Approved OMB No. 0704-0188		
Public reporting burden for the collection of information is estimated to average 1 hour per response, including the time for reviewing instructions, searching existing data sources, gathering and maintaining the data needed, and completing and reviewing the collection of information. Send comments regarding this burden estimate or any other aspect of this collection of information, including suggestions for reducing this burden, to Washington Headquarters Services, Directorate for Information Operations and Reports, 1215 Jefferson Davis Highway, Suite 1204, Arlington VA 22202-4302. Respondents should be aware that notwithstanding any other provision of law, no person shall be subject to a penalty for failing to comply with a collection of information if it does not display a currently valid OMB control number.					
1. REPORT DATE 29 JUN 2000		2. REPORT TYPE		3. DATES COVERED 00-00-2000 to 00-00-2000	
4. TITLE AND SUBTITLE Electromagnetic Induction and Magnetic Sensor Fusion for Enhanced UXO Target Classification				5a. CONTRACT NUMBER	
				5b. GRANT NUMBER	
				5c. PROGRAM ELEMENT NUMBER	
6. AUTHOR(S)				5d. PROJECT NUMBER	
				5e. TASK NUMBER	
				5f. WORK UNIT NUMBER	
7. PERFORMING ORGANIZATION NAME(S) AND ADDRESS(ES) Naval Research Laboratory, Washington, DC, 20375-5320				8. PERFORMING ORGANIZATION REPORT NUMBER	
9. SPONSORING/MONITORING AGENCY NAME(S) AND ADDRESS(ES)				10. SPONSOR/MONITOR'S ACRONYM(S)	
				11. SPONSOR/MONITOR'S REPORT NUMBER(S)	
12. DISTRIBUTION/AVAILABILITY STATEMENT Approved for public release; distribution unlimited					
13. SUPPLEMENTARY NOTES					
14. ABSTRACT					
15. SUBJECT TERMS					
16. SECURITY CLASSIFICATION OF:			17. LIMITATION OF ABSTRACT Same as Report (SAR)	18. NUMBER OF PAGES 41	19a. NAME OF RESPONSIBLE PERSON
a. REPORT unclassified	b. ABSTRACT unclassified	c. THIS PAGE unclassified			

Contents

Figures.....	v
Tables.....	vi
1. Introduction.....	1
1.1 Background Information.....	1
1.2 Official DOD Requirement Statement.....	2
1.3 Objective of the Demonstration.....	2
1.4 Regulatory Issues.....	2
1.5 Previous Testing of the Technology.....	2
2. Technology Description.....	3
2.1 Background and Applications.....	3
2.2 Strengths, Advantages, and Weaknesses of the Technology.....	5
2.3 Factors Influencing Cost and Performance.....	6
3. Site/Facility Description.....	6
3.1 Background.....	6
3.2 Site Characteristics.....	7
4. Demonstration Approach.....	8
4.1 Performance Objectives.....	8
4.2 Physical Setup and Operation.....	8
5. Performance Assessment.....	9
5.1 Performance Data.....	9
5.1.1 Requirements Demonstration.....	9
5.1.2 Final Demonstration.....	14
5.2 Data Assessment.....	19
5.3 Technology Comparison.....	20
6. Cost Assessment.....	23
6.1 Cost Performance.....	23
7. Technology Implementation.....	24
7.1 DoD Need.....	24
7.2 Transition.....	24
8. References.....	25

Appendix A. Points of Contact.....	27
Appendix B. Data Archiving and Demonstration Plan.....	29
Appendix C. <i>MTADS</i> Target Report from the Final Demonstration	31

Figures

Figure 1. Magnetic field transmitted by the <i>MTADS</i> array.....	4
Figure 2. Road map showing the location of Blossom Point.....	7
Figure 3. Aerial view of Blossom Point, MD with "L" Range highlighted.....	7
Figure 4. Survey tracks over an 81-mm mortar.	10
Figure 5. Measured response and model fits from the 81-mm mortar.....	10
Figure 6. North-South EM survey of the Test Field.	11
Figure 7. Ternary plots of model-derived betas from the Test Field.	13
Figure 8. ROC curve generated from the 3β analysis at the Test Field.....	14
Figure 9. Examples of the items remediated during the Final Demonstration of the program.....	15
Figure 10. Results of three-beta fits for 81-mm mortars in the Final Demonstration	16
Figure 11. Results of three-beta fits for all other recovered targets.....	17
Figure 12. ROC curve for the detection of 81-mm mortars from the Final Demonstration	18
Figure 13. ROC curve for the detection of all ordnance from the Final Demonstration	18
Figure 14. Results of three beta fits for all targets with ellipses for each ordnance class	19
Figure 15. Results of Monte Carlo simulation considering several noise sources	21
Figure 16. ROC curves comparing three-beta analysis with magnetometer "size"	22

Tables

Table I. Model Fits and Trial Classification of Target Shape for Sample Test Field Targets.....	12
Table II. Model Fits for the four 3" d x 12" l Steel Cylinder at the Test Field.....	13
Table III. Size Distributions used in Magnetometer Analysis of the Final Demonstration.....	22
Table IV. Estimated Costs for a Hypothetical 200-Acre Survey Using These Methods.....	23

Electromagnetic Induction and Magnetic Sensor Fusion for Enhanced UXO Target Classification

Naval Research Laboratory

29 June 2000

1. Introduction

1.1 Background Information

Buried unexploded ordnance, UXO, is one of the Department of Defense's most pressing environmental problems. Not limited to active ranges and bases, UXO contamination is also present at DOD sites that are dormant and in areas adjacent to military ranges that are under the control of other government agencies and the private sector.

Traditional methods for buried UXO detection, characterization and remediation are labor-intensive, slow and inefficient. Typical detection and characterization methods rely on hand-held detectors operated by explosive ordnance disposal (EOD) technicians who slowly walk across the survey area. This process has been documented as inefficient and marginally effective.¹ In addition, a large portion, approaching 70% in some cases, of the total budget of a typical remediation effort is spent on digging targets that do not turn out to be UXO.

The Environmental Security Technology Certification Program, ESTCP, has supported the Naval Research Laboratory in the development of the Multi-sensor Towed Array Detection System, *MTADS*, to address these deficiencies. The *MTADS* incorporates both cesium vapor full-field magnetometers and pulsed-induction sensors in linear arrays that are towed over survey sites by an all-terrain vehicle. Sensor positioning is provided by state-of-the-art Real Time Kinematic (RTK) GPS receivers. The survey data acquired by *MTADS* is analyzed by an NRL-developed Data Analysis System (DAS). The DAS was designed to locate, identify and categorize all military ordnance at its maximum self-burial depth. It is efficient and simple to operate by relatively untrained personnel.

The performance of the *MTADS* has been demonstrated at a number of prepared sites and live ranges over the past two years.²⁻¹¹ It can detect and locate ordnance with accuracies on the order of 15 cm.⁵ However, even with careful mission planning and preliminary training there are still

significant numbers of non-ordnance targets selected. Thus, more effective discrimination algorithms are required. This program was designed to exploit the dependence on target shape of the pulsed-induction response to enhance the discrimination capability of MTADS.

1.2 Official DOD Requirement Statement

The Navy Tri-Service Environmental Quality Research Development Test and Evaluation Strategic Plan specifically addresses under Thrust Requirements 1.A.1 and 1.A.2, the requirements for improved detection, location and removal of UXO on land and under water. The index numbers associated with these requirements are 1.I.4.e and 1.III.2.f. The priority 1 rankings of these requirements indicate that they address existing statutory requirements, executive orders or significant health and safety issues. Specifically the requirements document states:

There are more than twenty million acres of bombing and target ranges under DOD control. Of particular concern for the Navy are the many underwater sites which have yet to be characterized. Each year a significant fraction (200,000-500,000 acres) of these spaces is returned to civilian (Private or Commercial) use. All these areas must be surveyed for buried ordnance and other hazardous materials, rendered certified and safe for the intended end use. This is an extremely labor intensive and expensive process, with costs often far exceeding the value of the land.... Improved technologies for locating, identifying and marking ordnance items must be developed to address all types of terrain, such as open fields, wooded areas, rugged inaccessible areas, and underwater sites.¹²

The MTADS addresses all aspects of the Tri-Service Requirements for land-based buried UXO. It is designed to survey large sites rapidly and efficiently, with commensurate economic benefits. Moreover, it is capable of detecting all classes of buried UXO at their likely self-burial depths. The system will correctly locate buried targets, determine their burial depths, classify the likely ordnance size, provide for future target way pointing, as well as create GIS-compatible target output maps and sorted target tables.

1.3 Objective of the Demonstration

This was the final demonstration of the modified MTADS incorporating the analysis techniques described below. We showed in the first demonstration of this program, the Requirements Demonstration conducted on the NRL Test Field at Blossom Point, that these methods are useful tools for target classification. This Final Demonstration was designed to use these tools on a real-world site and quantify the benefits obtained from their use.

1.4 Regulatory Issues

There were no external regulatory issues impacting this demonstration. All activities described here occurred on a government test range and were governed by a locally approved Health and Safety Work Plan.

1.5 Previous Testing of the Technology

An initial test of the technology described in this report, designated the Requirements Demonstration, was conducted in February 1999 at the NRL Test Site¹³ at the Blossom Point Facility. Results of that test will be described in following sections of this report.

2. Technology Description

2.1 Background and Applications

The standard *MTADS* technology has been described in detail previously.² Briefly, the system hardware consists of a low-magnetic-signature vehicle that is used to tow linear arrays of magnetometer and pulsed-induction sensors to conduct surveys of large areas to detect buried UXO. The *MTADS* tow vehicle, manufactured by Chenoweth Racing Vehicles, is a custom-built off-road vehicle, specifically modified to have an extremely low magnetic signature. Most ferrous components have been removed from the body, drive train and engine and replaced with non-ferrous alloys.

The *MTADS* magnetometers are Cs-vapor full-field magnetometers (Geometrics Model 822ROV). An array of eight sensors is deployed as a magnetometer array. The time-variation of the Earth's field is measured by a ninth sensor deployed at a static site removed from the survey area. These data are used to correct the survey magnetic readings. The pulsed-induction sensors (specially modified Geonics EM-61s) are deployed as an overlapping array of three sensors. The sensors employed by *MTADS* have been modified to make them more compatible with vehicular speeds and to increase their sensitivity to small objects.

The sensor positions are measured in real-time (5 Hz) using the latest RTK GPS technology. All navigation and sensor data are time-stamped and recorded by the data acquisition computer in the tow vehicle. The DAS contains routines to convert these sensor and position data streams into anomaly maps for analysis.

The standard *MTADS* analysis method has also been described previously.¹⁴ The magnetometry data has been very successfully modeled using a dipole response. We routinely recover target x,y positions to within 15 cm and target depths to $\pm 20\%$.⁵ Within the signal to noise ratio of the *MTADS*, we see no residual signature attributable to higher moments.¹⁴ The pulsed-induction modeling has been less successful. The standard algorithm is based on a sphere model and does not well represent the signatures we obtain. We have discussed the deficiencies of this model and proposed an ordnance model based on a prolate spheroid.¹⁴

This program was organized around the premise that classification based on shape is central to the problem of discriminating between unexploded ordnance (UXO) and clutter. Most UXO fit a specific profile: they are long and slender with typical length-to-diameter aspect ratios of four or five. Many clutter items, on the other hand, do not fit this profile. Using pulsed-induction sensor data, we have developed a model-based estimation procedure to determine whether or not a target is likely to be a UXO item. The model relies on exploiting the dependence of the induced field on target size, shape and orientation.

The EM61 is a time domain instrument. It operates by transmitting a magnetic pulse that induces currents in any nearby conducting objects. These currents produce secondary magnetic fields that are measured by the sensor after the transmitter pulse has ended. The sensor response is the voltage induced in the receiver coil by these secondary fields, and is proportional to the time rate of change of the magnetic flux through the coil. The sensor integrates this induced voltage over a fixed time gate and averages over a number of pulses. An illustration of the magnitude and

direction of the field transmitted by the *MTADS* array is shown in Figure 1. Note that the field experienced by an object directly below the array is substantially different than an object in front or behind the array. The implications of this for target signatures will be seen in Section 5 of this report.

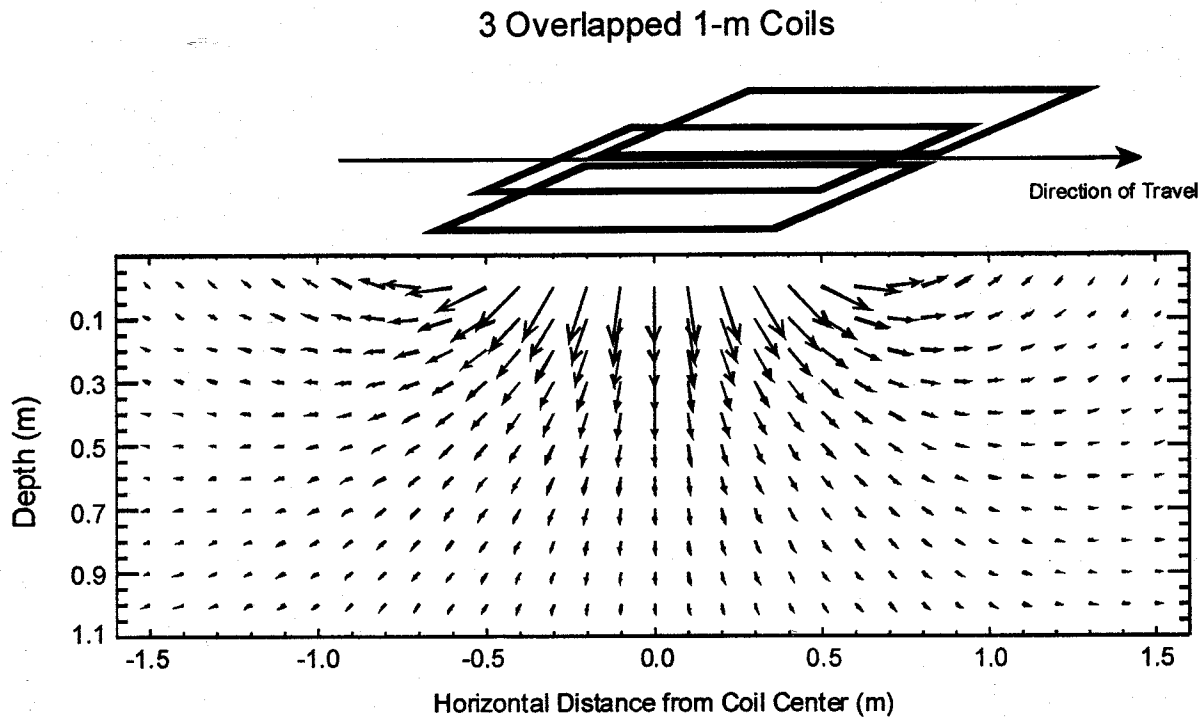


Figure 1 – Direction and magnitude of the magnetic field transmitted by the *MTADS* EM-61 array.

The model to be used in this demonstration has been jointly developed by NRL and AETC, Inc. and has been described recently.^{14,15} Briefly, it relies upon the fact that the EM61 signal is a linear function of the flux through the receiving coil. The flux is assumed to originate from an induced dipole moment at the target location given by:

$$\mathbf{m} = \mathbf{UBU}^T \cdot \mathbf{H}_0 \quad (1)$$

where \mathbf{H}_0 is the peak primary field at the target, \mathbf{U} is the transformation matrix between the coordinate directions and the principal axes of the target, and \mathbf{B} is an empirically determined, effective magnetic polarizability matrix. For any arbitrary compact object, this matrix can be diagonalized about three primary body axes and written as:

$$\mathbf{B} = \begin{bmatrix} \beta_x & 0 & 0 \\ 0 & \beta_y & 0 \\ 0 & 0 & \beta_z \end{bmatrix} \quad (2)$$

The relative magnitudes of these β 's are determined by the size, shape, and composition of the object as well as by the transmit pulse and fixed time gate of the EM61. Different time gates may result in different values and different relative values of these β 's for a given object. The transformation matrix contains the angular information about the orientation of these body axes.

For an axisymmetric object, B is a diagonal tensor with only two unique coefficients, corresponding to the longitudinal (β_l) and transverse (β_t) directions:

$$B = \begin{bmatrix} \beta_l & 0 & 0 \\ 0 & \beta_t & 0 \\ 0 & 0 & \beta_t \end{bmatrix} \quad (3)$$

Empirically, we observe that for elongated ferrous objects such as cylinders and most UXO, the longitudinal coefficient is greater than the transverse coefficient. For flat ferrous objects such as disks and plates, the opposite is true. This matches the behavior of these objects in the magnetostatic limit. For non-ferrous objects such as aluminum cylinders and plates, these relationships are reversed.

We tested several implementations of this model in the Requirements Demonstration. All were designed to take advantage of the fact that we obtain reliable position (x,y,z) information from the magnetometer signals. We then fitted the pulsed-induction response to models with combinations of two or three response coefficients, β , and two or three orientation angles. One of the goals of the Requirements Demonstration was to determine which of these models resulted in the most classification utility with the least data collection expense. As we will discuss below, we have determined that collecting two orthogonal EM surveys and fitting the data using the three β , three angle model yields the optimum results. This is the survey methodology that was used in this Demonstration.

2.2 Strengths, Advantages, and Weaknesses of the Technology

No single method currently available will be the "magic bullet" of classification. We have already demonstrated^{5,7} that an impressive level of discrimination is possible using the standard *MTADS* if a small training area is investigated prior to data analysis on the entire site and the distribution of ordnance is limited. This discrimination is based primarily on fitted dipole "size." In this program we have demonstrated methods designed to add an extra "dimension" to the discrimination, that of "shape." For items of the same induced magnetic dipole we can discriminate based on the ratio of responses of the items three axes to the EM induction sensors in the *MTADS* suite. As we will show in a later section, this adds some discrimination capability to the system.

Even with the most optimistic result however, these methods will not result in a perfect system. As we have stated above, this program is based on the idea of classification by shape. By definition, this implies that clutter items that have similar shapes to ordnance will be classified as ordnance. Items such as pipes and post sections are representative of this problem. If it is important to reduce remediation costs to the extent that these items are not dug, other methods,

possibly sensitive to composition or the presence of explosive compounds, will have to be employed in conjunction with those being developed in this program.

2.3 Factors Influencing Cost and Performance

Implementation of the methods developed in this program requires additional survey time compared to a minimum detection survey. We have previously demonstrated that, in many cases, the *MTADS* can detect essentially all UXO with a total-field magnetometry survey. For ordnance target sets that include 60- and 81-mm mortars at depths of 0.75 to 1 m an overlapping EM induction survey is required to get a high detection probability. With the current *MTADS* EM array configuration, we require two orthogonal EM surveys to ensure sufficient "illumination" of each target to get a reliable fit to the model presented in this report. This increases the survey hours on-site considerably although it does not impact the mobilization and data analysis costs. In many cases, these extra costs are only equivalent to the cost of digging one or two targets per acre.

3. Site/Facility Description

3.1 Background

The Requirements Demonstration was performed at the Naval Research Laboratory Ordnance Classification Test Site located on the Army Research Laboratory's Blossom Point Research Facility. This site was designed¹³ to contain a variety of ordnance, ordnance simulants and clutter at known positions and orientations for algorithm development and testing. The Final Demonstration was performed on a live range at the Blossom Point Facility, the "L" Range.

During World War II, Harry Diamond and his team at the National Bureau of Standards (NBS, now named NIST) needed open areas where they could test the fuzes they were developing. They established test sites at Aberdeen Proving Ground, MD, Fort Fisher, NC and in early 1943 NBS leased land and established a proving ground for proximity fuzes at Blossom Point. By September 1945, 14,000 rocket and mortar rounds had been fired. In 1953, the lease on the property was transferred to the Army, which operated the property as a fast-reaction, low-cost range for experimental work. Firing ranges provided a 2000-yard maximum range for land impact and a 10,000-yard maximum for water impact. During the Vietnam War, the Army's Harry Diamond Laboratory was very active at the site.

The "L" Range is the main range for impact testing of various munitions at Blossom Point. It is approximately 800 feet wide by 5000 feet long and encompasses ~93 acres. This range has been the primary impact area throughout the history of the site. Some of the known firings include 81-mm mortars in 1961, 2.75-inch rockets fired from helicopters throughout the 70's, and various listings of 60-mm mortars, 75-mm projectiles, 81-mm mortars and various barrage rockets.

HFA, Inc. conducted an ordnance removal at the Blossom Point Test Facility in 1996.¹⁷ Two sites were cleared in conjunction with utility work and construction. Two sites totaling 66 acres were cleared; one a clear area parallel to "L" range and one a wooded area north of the first.

The area was excavated to 4 feet on the construction sites and 2 feet for the utility lines. Seven hundred fifty three UXO items and 9,267 lbs. of scrap were removed from the site. The UXO consisted of a wide variety of ordnance types and classes with a preponderance of 20- and 30-mm rounds, 60- and 81-mm mortars, and 4.2-in rockets. This is consistent with the firing records mentioned above.

3.2 Site Characteristics

Figure 2 is a road map of a portion of Charles County, Maryland showing the location of Blossom Point relative to La Plata, the County Seat. Figure 3 is an aerial photo of the Blossom Point Field Facility with the area comprising the Final Demonstration test site highlighted.

The Demonstration area is located on high ground, well above the surrounding rivers. The site has good sky view for GPS but is bordered by a densely wooded area that is ideal for testing non-GPS location systems.

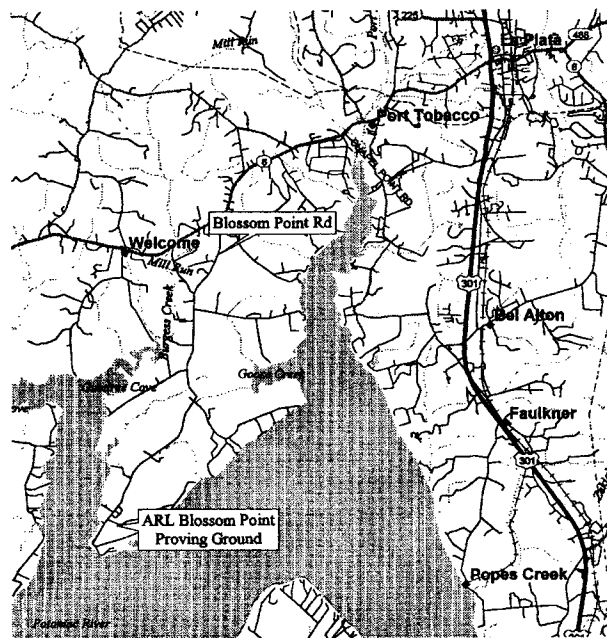


Figure 2 – Road map showing the location of Blossom Point.

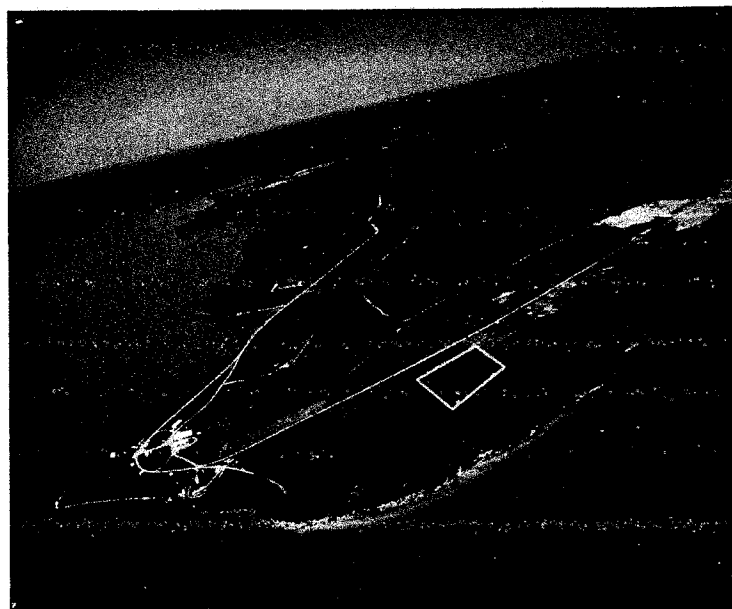


Figure 3 – Aerial view of Blossom Point, MD with the approximate location of the Demonstration Site on the Army Research Laboratory Blossom Point "L" Range highlighted.

4. Demonstration Approach

4.1 Performance Objectives

The objective of the Demonstration was to quantify the classification performance available using the *MTADS* array of modified, off-the-shelf pulsed-induction sensors and the data modeling algorithms developed in this program. The Demonstration proceeded in three phases: data collection, data analysis, and target marking and remediation.

Data collection consisted of surveying an approximately three-acre area on a live range, known to have had many detonations, using both the magnetometers and pulsed-induction sensor suites of *MTADS*. The magnetometer survey was conducted in an E-W orientation to minimize the effects of GPS signal loss at the woodline. The pulsed-induction survey was carried out both E-W and N-S to get the best possible "illumination" of each target.

Data analysis was accomplished using the *MTADS* Data Analysis System. The DAS has been upgraded during this program to simultaneously analyze a magnetometer and several pulsed-induction survey data sets. The analysis consists of fitting individual target signatures to the model discussed above to extract target position, size, and relative response along three orthogonal axes. These relative response coefficients were used to classify the target as UXO or scrap. This phase of the Demonstration resulted in a spreadsheet-like target report that included target number, location, depth, three response coefficients, and predicted class. This spreadsheet, and the reasoning behind the target assignments, was communicated to the Institute for Defense Analyses (IDA) before remediation was begun.

The final phase of the Demonstration consisted of remediation of the analyzed targets. We had planned to select approximately 200 targets for remediation. After analysis of the survey data we found that there were only ~200 targets in the survey area with signatures well enough separated to get a good model fit so no selection was necessary. This target set represents ~25% of those targets with magnetic anomaly > 50nT and/or EM anomaly > 70nT. In our view, this is a large enough fraction of the total targets to ensure that a representative sample of all targets was remediated. These targets were flagged and remediated by a commercial UXO firm.

4.2 Physical Setup and Operation

Since this Demonstration was conducted on the Blossom Point site adjacent to where our equipment is housed, many of the normal pre-survey logistics such as establishment of first-order GPS markers, transport of the equipment to the site, and equipment setup and testing were not required. We performed the Demonstration "out of the garage." In all other ways, this Demonstration was conducted in accordance with our normal survey practices. The actual demonstration schedule was:

Date	Activity	Required Time
29 July 1999	Magnetometer Survey of Fusion Site and Man-portable Extension.	2 hrs Survey Time
3 August 1999	East-West EM Survey of Fusion Site and MP Extension.	5 hrs Survey Time
	North-South EM Survey of a portion of the Fusion Site	1 hr Survey Time
4 August 1999	North-South EM Survey of remaining Fusion Site and MP Extension.	4 hrs Survey Time
	Data Analysis and Target Classification	
12-13 August 1999	Flag Targets for Remediation.	16 Man Hours
16-18 August 1999	Target Remediation.	12 Man Days
26 August 1999	Required Demolition. 81 Shots on 73 Targets.	

5. Performance Assessment

Although not part of the Final Demonstration of this project, data will be presented in this section that was collected during the development of the algorithms and in the Requirements Demonstration in February 1999. These data will illustrate the performance of the model presented here under idealized conditions and will allow useful conclusions to be drawn about the performance degradation suffered when real-world sensor noise, location uncertainty, and finite target density are encountered.

5.1 Performance Data

5.1.1 Requirements Demonstration

The NRL Ordnance Classification Test Site contains a series of ferrous and non-ferrous shapes, selected clutter items and inert ordnance buried at known locations, orientations, and depths.¹³ During development of the model, EM induction signatures were acquired for many of the items to be emplaced in the test field on a laboratory jig that held the items in precisely known positions and orientations. During the Requirements Demonstration, survey data were collected on the test field using a variety of deployment approaches and *MTADS* EM array orientations to determine the most cost-effective approach for classification. For the purposes of this report, we will only consider the data set that consists of combined N-S and E-W survey lines. The results obtained from other combinations of survey conditions are similar.

As an illustration of the performance of the model developed in this work compared to the sphere model which is the basis of the initial *MTADS* DAS, let us focus on one of the targets in the test field, an 81-mm mortar at 0.5 m depth. The individual survey tracks over this target are shown in Figure 4. At each of the locations shown, a reading is acquired from the sensors. The measured data and model fits from the 3β model and the sphere model are shown in Figure 5 for each of the two surveys. As can be seen in the left-hand panel of the Figure, the signature from a

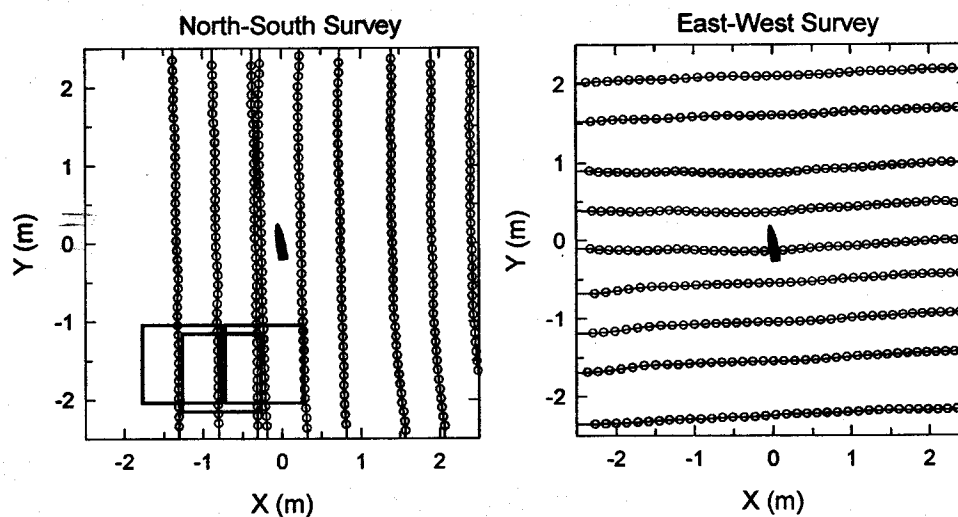


Figure 4 – *MTADS* survey tracks over an 81-mm mortar placed parallel to the surface at a depth of 0.5 m. The right sensor is represented by green symbols, the center by black and the left by red.

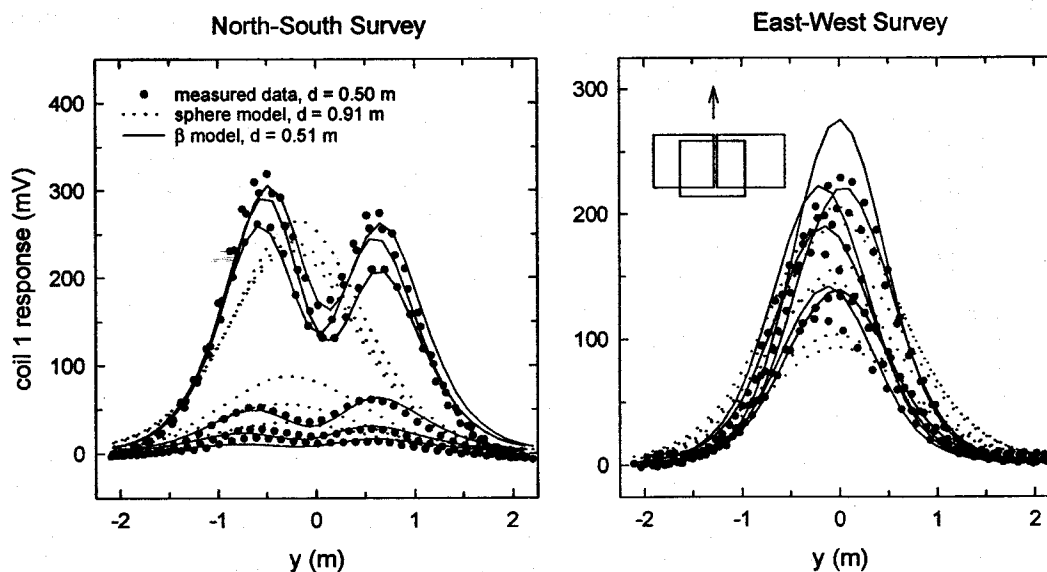


Figure 5 – Measured response and model fits using both the sphere model and the 3β model developed for this program for an 81-mm mortar at 0.5 m. The color scheme for the three sensors in the *MTADS* array is as in Figure 4.

target oriented along track is the now familiar double-humped shape. This arises from the varying coupling of the transmitted pulse, as shown in Figure 1, with the target. As the array approaches a target oriented along track, the coupling with the long axis of the target is strong, although the distance is large, and the signal is large. Directly over the target, the coupling is to the short axis of the target and the signal is relatively weak. Of course, the sphere model can not reproduce this asymmetry. The right-hand panel depicts the target oriented across track. Here the sphere model can reproduce the observed shape but the fitted depths are not correct. The results are similar for the mortar placed vertically; the shape is symmetric but the sphere model does not return the correct depth.

An overview of the entire Test Field is shown in Figure 6. The measured anomalies associated with each of the 61 targets in the test field were isolated and fit to the model as above. Sample

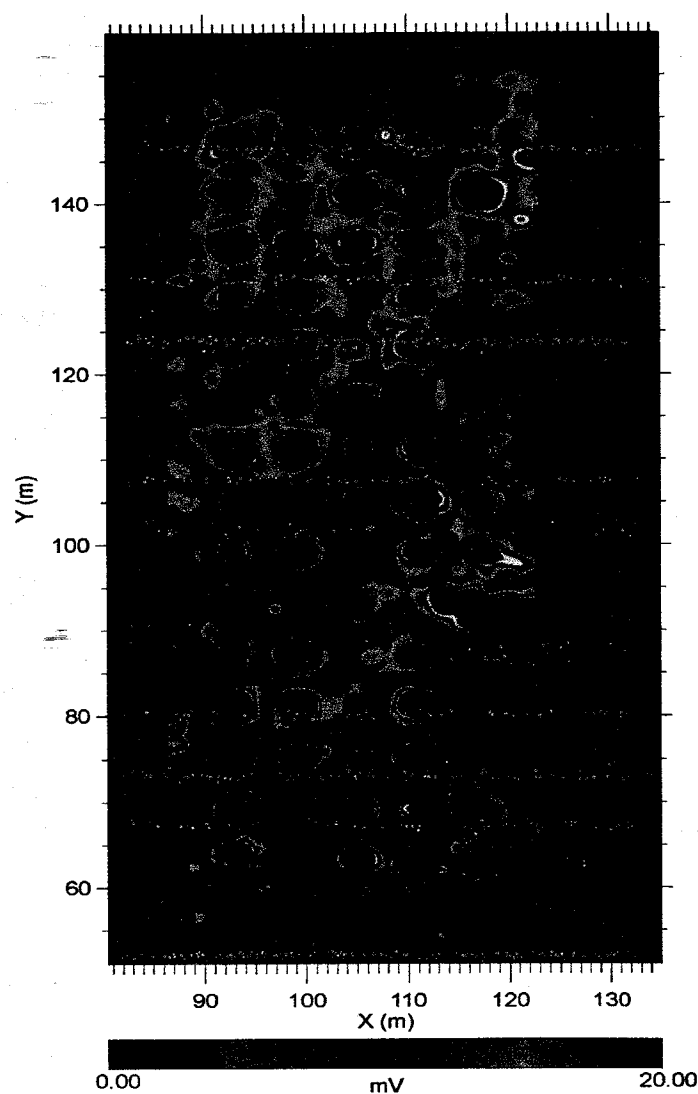


Figure 6 – North-South EM survey of the Test Field.

fit results for various test shapes are presented in Table I. Two goals of this test were to determine how the beta coefficients varied with object shape and how much measurement errors would effect the absolute and relative values of the fitted betas compared to those obtained in a static jig test of the items emplaced in the test field.

Table I. Model Fits and Trial Classification of Target Shape for Sample Test Field Targets

Item	β_1	β_2	β_3	Classification.
3"d x 6"l steel cylinder	2.063	1.195	1.100	LONG
3"d x 12"l steel cylinder	5.74	2.76	2.526	LONG
3"d x 24"l steel cylinder	8.634	4.475	3.828	LONG
8" x 8" x 1/4" square steel plate	4.954	4.577	1.499	FLAT
4" x 4" x 1/4" square steel plate	1.142	0.906	0.303	FLAT
12" x 3" x 1/4" rectangular steel plate	3.427	0.796	0.422	LONG
4.8"d steel sphere	3.093	2.217	2.029	LONG
81-mm Mortar	5.373	0.842	0.721	LONG
Shovel Blade	6.315	5.806	3.386	FLAT

Depending on these two factors, it was initially thought that significant discrimination could be achieved by simply relating the relative betas directly to object shape, i.e. $\beta_1 > \beta_2 \approx \beta_3$ implies a long, ordnance shape and $\beta_1 \approx \beta_2 > \beta_3$ implies a flat, debris shape. Overall, we correctly classified 33 of the 34 targets that were ordnance or ordnance simulants as being long and 10 of the 25 plate and clutter items as being flat. Thus, using this model we are able to avoid identifying 40% of the debris as ordnance (false positives) while only missing one ordnance item (false negative) in this idealized test field.

One problem identified with this simple shape based discrimination arises with rectangular plates. Despite the distinct relative dimensions of the 12" x 3" x 1/4" plate in Table I, the range of measured betas does not directly reflect this: 3.427:0.796:0.422. The relative betas are more indicative of a long, ordnance type item than flat, clutter item.

The variability of the fitted betas for one of the test targets, a 3"d by 12"l steel cylinder, at different depths and orientations is shown in Table II. For each beta, there is a 20-30% variation about the mean. Related to this is the fit result for a steel sphere in Table I. While it is expected that the fitted betas should be equal, they are not. The range in the three values is again roughly 25% about the mean. This variation presumably arises from measurement error (sensor noise and positioning error) and it places a limit on how well the relative beta values can be used to discriminate shape based on relative values and individual objects based on absolute values.

Table II. Model Fits for the four 3" D x 12" L Steel Cylinder at the Test Field

β_1	β_2	β_3	Depth (m)	Orientation
5.740	2.760	2.526	0.35	Horizontal
3.918	2.733	2.051	0.35	Vertical
3.822	2.052	1.804	0.5	Horizontal
6.297	1.777	1.058	0.5	Vertical

This variability in relative betas is illustrated in Figure 7. The left-hand panel of the figure is a ternary plot of the betas derived from measurements on the test field objects on a test jig fit assuming axial symmetry. We did not collect enough data at this time to allow a fit without assumption of symmetry. As expected, the long symmetric objects (cylinders and ordnance) exhibit one large beta and two smaller betas and the plates have one small and two large betas responses. The right-hand panel shows the same plot for betas derived from the fits to the survey data. The effect of sensor noise and location uncertainty is to broaden the long objects off the diagonal and partially confuse them with the rectangular plates.

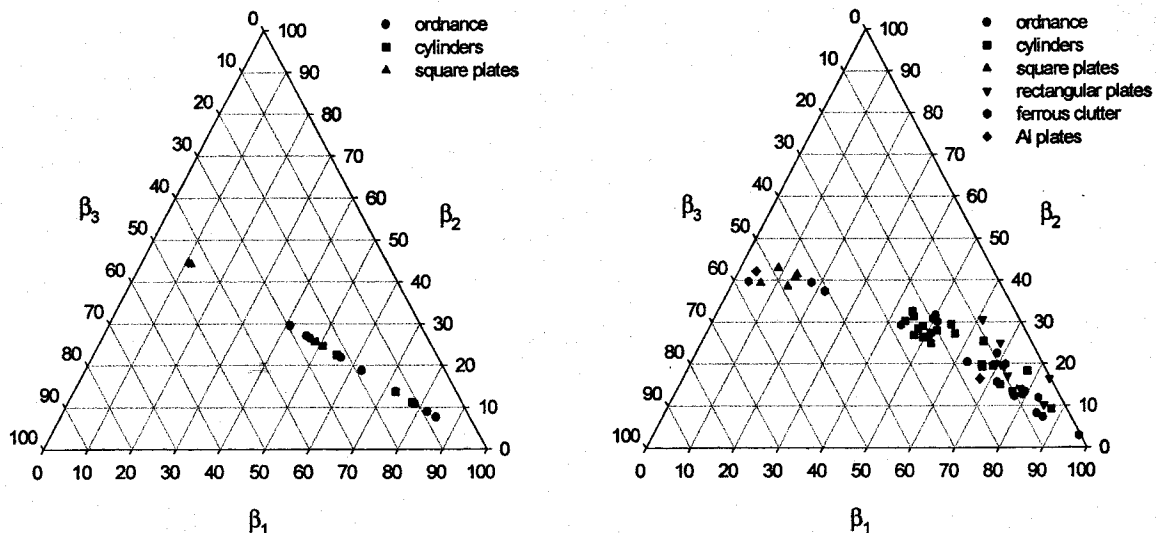


Figure 7 – Ternary plots of the relative values of the three betas derived from fits of measured signatures. The left-hand panel is the result of measurements in a test jig. The right-hand panel results from field measurements and shows the effects of measurement errors as discussed in the text.

One measure of performance in detection and discrimination problems is a Receiver Operating Characteristic (ROC) curve. These curves plot the probability of detection (P_D) versus the probability of false alarm (P_{FA}) as some threshold of detection is varied. In the case of ordnance/clutter discrimination, the curve plots the probability of correctly identifying an ordnance item as ordnance versus the probability of incorrectly identifying a clutter item as ordnance. The threshold level that is varied is the range of the discriminating fit parameter. A

ROC curve for this analysis methodology can be generated by creating an area with $\beta_1 > 40$ and $\beta_2 \approx \beta_3$ and then progressively expanding the width of this area. This ROC curve is shown in Figure 8. Approximately one third of the false alarms can be eliminated without reducing P_D .

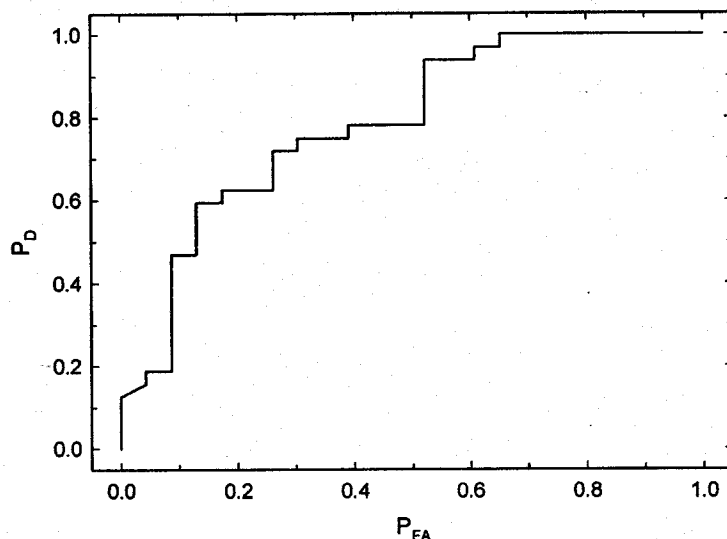


Figure 8 – ROC curve generated using 3β analysis on the survey data from the Ordnance Classification Test Field.

For all 61 targets in the test field the model-derived locations were a fraction of the data spacing (0.15m along track and 0.5m sensor separation). Depth estimates were a fraction of the object size. For most targets the derived orientations agreed well with the known values. The exceptions were symmetric objects oriented vertically. These targets should have a symmetric anomaly. At the time these data were collected, we had a small timing error among the three sensors in the array. The result of this timing error was to introduce some artifact asymmetry into the anomalies. This timing error has since been eliminated.

5.1.2 Final Demonstration

After completion of a magnetometer and two EM surveys in perpendicular directions, 201 targets were analyzed and marked for remediation on the L Range Final Demonstration site. An abbreviated version of the *MTADS* target report for these items is attached as Appendix C. A more complete version of the report with positions in absolute coordinates and the results of the trial 2β analysis has been provided to IDA and is available from the authors.

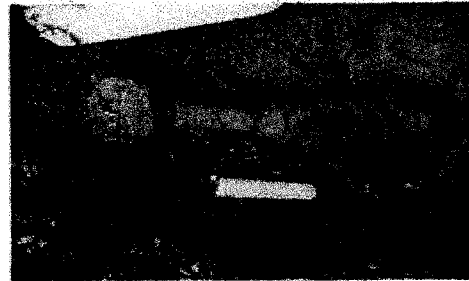
A total of 188 targets were recovered from this test area. Examples are pictured in Figure 9. There were 66 ordnance items, 20 ordnance related items, 66 exploded fragments, and 36 items not related to ordnance. The ordnance items broke down into three groups: 48 81-mm mortars, 8 mortars of smaller sizes, and 10 miscellaneous ordnance items. The miscellaneous items included 2 bomb fuzes, a 76mm projectile, and two 5-in rockets. The ordnance related items were rocket motors with fins and mortar tail booms. The exploded fragments appeared to be



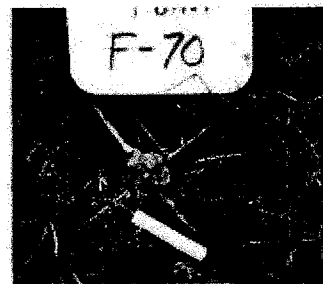
5-in rocket



81-mm



61-mm



rocket motor



frag



non-ordnance

Figure 9 – Examples of the items remediated during the Final Demonstration of the program.

mostly from mortars. The non-ordnance items included cable tie down points for test towers that had been removed, block and tackles from the cables, and a variety of odd scraps of metal (rebar, sheet metal, angle iron, and bolts). We will concentrate our initial discussion on the 81-mm mortars as they provide the best fit statistics. After remediation, three of what proved to be 81-mm's (targets 166, 171, and 178) were found to have 3β fits in which the primary β was very large and one of the secondary β 's was near zero. Re-inspection of the survey data showed that this resulted from a large zero offset between the two perpendicular survey tracks. After correcting for this offset, reasonable β fits were obtained for these objects. The parameters of these corrected fits are listed in Appendix C and used in the analysis that follows.

The results of the three-beta fits for the 81-mm's are shown in Figure 10. The values of the primary beta (largest) are plotted on the x-axis. The two smaller betas are plotted on the y-axis, where the symbol in the plot represents the average of the two and the vertical line represents the spread between the two values. We want to preserve the magnitude of beta, which was lost in the ternary plots used above. We find this to be an easier way to visualize the spread in the data than plotting the points in three dimensions. Note that if the fit results were perfect (no measurement errors) then the data would all be symbols with no vertical line (secondary betas are equal for axisymmetric objects).

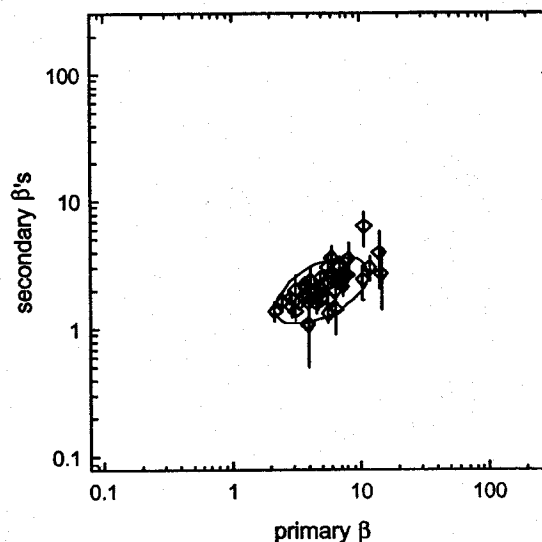


Figure 10 – Two-dimensional representation of the three beta fits for the 81-mm mortars in the Final Demonstration. The value of the primary beta (largest) is plotted on the x-axis. The two smaller betas are plotted on the y-axis, where the symbol represents the average and the vertical line represents the spread.

The three beta values are best described by a log-normal distribution. In logarithmic quantities, the mean is 0.6970, 0.3183, and 0.3098 with standard deviations of 0.2, 0.09, and 0.13 for β_1 , β_2 , and β_3 respectively. In measured units, this corresponds to an average response of 4.98 along the length of the mortar and 2.0 transverse to this. Note that the value range from 2 to 12 along the primary axis, which is much greater than the 20-30% observed for objects in the test field. It is

thought that this enlarged spread is largely due to positioning errors in height as the array is towed over the uneven ground of a live site. We will discuss this point in more detail later in the report. The ellipse plotted in Figure 10 represents a three dimensional ellipsoid with major and minor radii that are equal to two standard deviations of the primary and secondary betas. The ellipse is tilted because of a weak correlation between the primary versus the secondary betas (stronger primary betas have stronger secondary betas). As we will show below, this ellipsoidal curve can be used to calculate the probability that a given beta fit represents an 81-mm mortar.

The three beta fit results from the other ordnance items recovered at the L Range are plotted in the left panel of Figure 11. The approximate primary versus secondary beta values range from 0.7/0.5 for the bomb fuze to 178.0/62.0 for the 5-in rockets. A similar plot for the fragments, the ordnance related scrap, and the non-ordnance scrap is presented in the right panel of Figure 11. It is interesting to note that the bulk of the fragments do not overlap the 81-mm mortars. One would expect that a large spread in the secondary betas should result from an irregularly shaped object. Overall, the spread observed in the right panel of Figure 11 is not much worse than the spread for the axisymmetric ordnance objects (Figure 10 and left panel of Figure 11). After examining photos of the objects dug, this is not too surprising. Most of the scrap is to first order elongated, with approximately equal secondary dimensions.

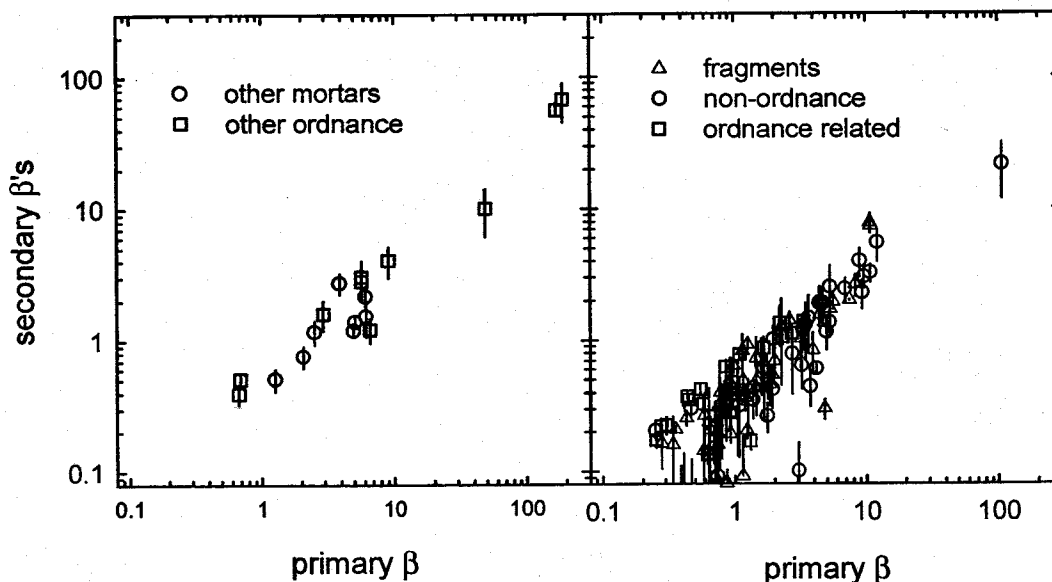


Figure 11 – Two-dimensional representation of the three beta fits for targets from the Final Demonstration plotted as in Figure 10. The left panel shows the results for all other ordnance recovered from the site, and the right panel those for the scrap and clutter recovered.

Examples of ROC curves based on the L-Range data are shown in Figures 12 and 13. To generate these curves, the ellipsoid in Figure 10 is grown larger (in three dimensions) and the number of ordnance (PD) and non-ordnance (FA) betas that fall within this three dimensional region are counted. Figure 12 plots the results for a single 81-mm ellipsoid. In Figure 13, ellipsoids are generated about each of the ordnance items present. The sizes of these ellipsoids

are grown uniformly based on the standard deviations and correlations of the 81-mm betas; too few of these other ordnance items were fitted to generate valid beta statistics. This is illustrated on the familiar beta plot in Figure 14.

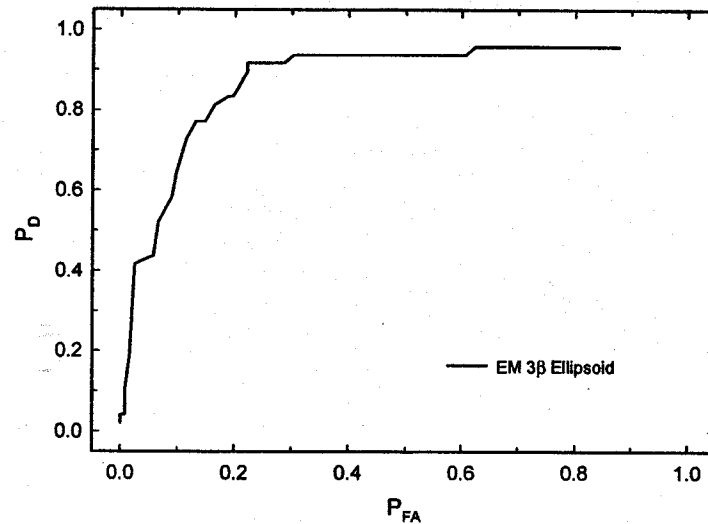


Figure 12 – ROC curve for the detection of 81-mm mortars from the Final Demonstration

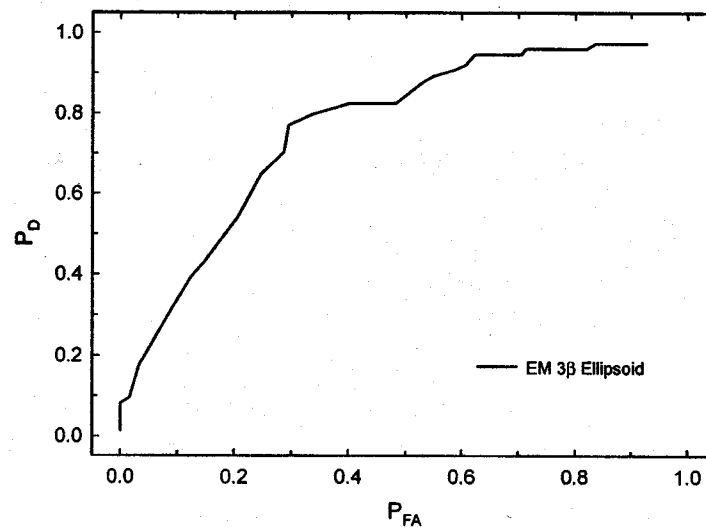


Figure 13 – ROC curve for detection of all ordnance at the Final Demonstration

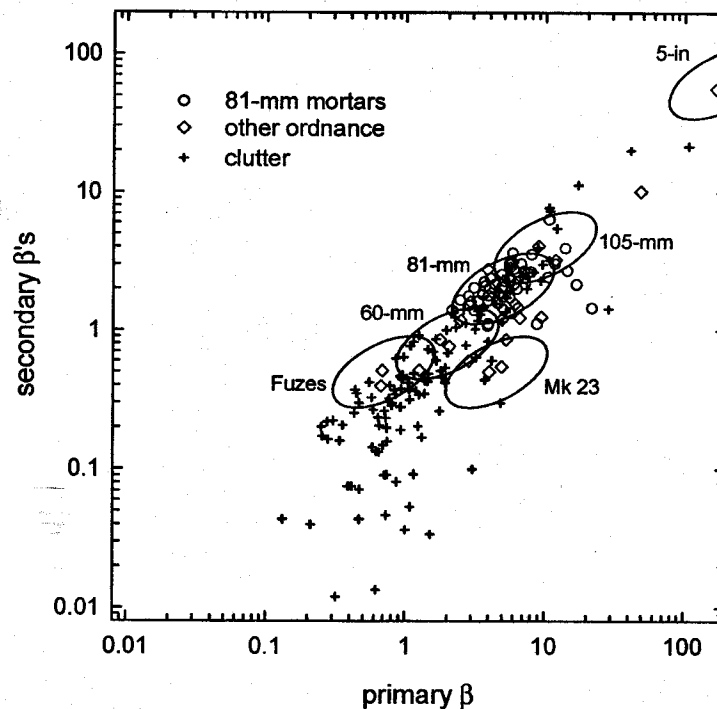


Figure 14 – Two-dimensional representation of the three beta fits to all targets from the Final Demonstration with ellipses for each ordnance class derived from the 81-mm mortar ellipse

The discrimination performance for a single ordnance item, 81-mm mortars, matches that observed in the test field. We achieve a roughly 40% reduction in false alarms without impacting P_D . The story is more complicated when trying to discriminate several classes of ordnance from the background clutter, Figure 13. In order to identify the small fuzes in this field as ordnance, a large number of clutter items have to be included. In part, this is the inevitable result of trying to discriminate ordnance ranging in size from fuzes to 5-in rockets from clutter. This difficulty may be mitigated by obtaining more data, hence better fit statistics, on the smaller ordnance items. Using the error ellipsoid derived from the distribution of 81-mm mortar fits, as we were forced to do, may well overstate the region of the 3-D space occupied by the smaller ordnance items. As we obtain more model fits to remediated ordnance and improve our fit statistics we will be able to test this notion.

5.2 Data Assessment

The survey data collected at the Final Demonstration of this program were of sufficient quality to meet the goals of the Demonstration. We were able to increase the discrimination available using *MTADS* EM induction survey data. Several features of the data limited the classification ability however. We showed in the Requirements Demonstration that sensor noise and sensor location error limited the estimated betas to a precision of ~25%. Some improvement is possible in this regard but not a lot. The GPS units used for sensor location on the *MTADS* array are state-of-the-art receivers with cm-level precision. Because of the response of the EM-61 sensors to the GPS antenna, the antenna is located ~1.5 m in front of the sensor array. Although the

antenna location is known to centimeters, there is some location uncertainty introduced by the back projection of the sensor locations from the antenna position. A two-antenna array, with a GPS antenna in front of and behind the EM sensors, would reduce sensor location uncertainties. At the time of this Demonstration, this would have involved the purchase of another independent GPS receiver/radio combination. Now, because of the demand from the mining and construction markets, dual antenna systems are available for a modest increase in price. Sensor noise is a different issue. Progress here requires a new generation of EM induction sensors.

Compared to the data collected during the Requirements Demonstration, there was a further decrease in the precision of the fitted beta values during the Final Demonstration. We attributed this above to vertical motion of the EM array over the rough ground at the live site. In an attempt to provide some quantitative underpinning to this assertion, we have performed a Monte Carlo simulation of the fitted response of an 81-mm mortar simulant with varying sources and magnitudes of noise. The object used in the simulation had a primary beta of 5 and two secondary betas of 2, about that expected for an 81-mm mortar. The object was placed at a distance of 0.6 m from the sensor array and given a random x,y position relative to the survey tracks and a random orientation. Each simulation included real *MTADS* GPS and sensor noise. The results of this simulation are shown in Figure 15. The top panel shows the results using only GPS and sensor noise. In this case, the fitted betas exhibit just the precision observed in the Requirements Demonstration, ~25%. For the simulation depicted in the bottom panel of Figure 15, a component of sensor height variation was added to simulate array bouncing over rough ground. We find that red noise with an RMS amplitude of 3 cm reproduces the spread in betas observed in the Final Demonstration. This is easily within the realm of possibility; the *MTADS* EM array platform does not have a suspension and is observed to bounce in rough terrain.

The terrain at the L Range demonstration was not especially rough for a live-site demonstration; *MTADS* has been demonstrated at several sites with much more challenging terrain. Therefore, to take advantage of the shape information inherent in the response of targets to the EM-61 array, better control of vertical displacements will be required. One option is to add suspension to the array platform. Another, possibly more effective, method would be to record the displacements of the array using inertial sensors and explicitly account for the position of the array in three dimensions in the data analysis procedure.

5.3 Technology Comparison

The obvious baseline for comparison of the value of the technology demonstrated here is the current *MTADS*. As mentioned above, the baseline *MTADS* is able to achieve a reasonable level of discrimination using magnetometry fits alone, especially when the ordnance distribution is limited. We will thus compare the results obtained in this demonstration with those that would be obtained by *MTADS* at the same site. To accomplish this, we have made use of the fitted mag "size" parameter that is included in the target report in Appendix C. For each ordnance class, we calculate a mean "size." Just as in the case of the 3-beta algorithm, we are able to calculate a distribution about this mean for the 81-mm mortars. We use the 81-mm distribution to generate a proportionally sized distribution for each ordnance class. The distributions derived are listed in Table III.

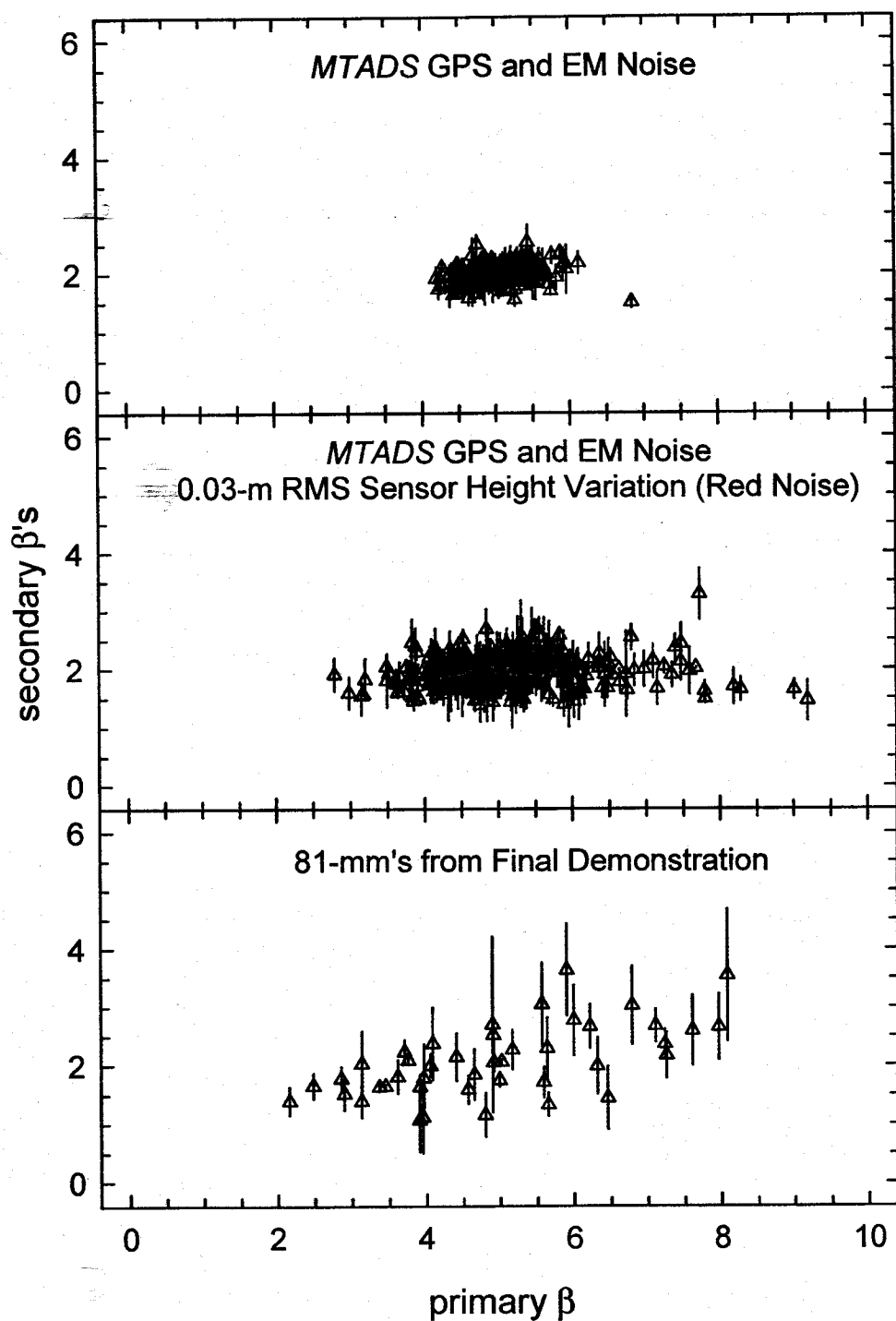


Figure 15 – Results of a Monte Carlo simulation of the fitted betas resulting from a range of model 81-mm mortars. The top panel includes *MTADS* GPS and sensor noise only. The middle panel adds vertical noise to simulate bouncing of the array over rough terrain. The lower panel shows results from the Demonstration for reference.

Table III – Size Distributions used in Magnetometer Analysis of the Final Demonstration

Ordnance Class	Size Distribution (mm)	Ordnance Class	Size Distribution (mm)
Fuzes	43 ± 9	81-mm mortar	76 ± 16
Mk23	56 ± 11	105-mm projectile	105 ± 21
60-mm mortar	60 ± 12	5" rocket	212 ± 42

We can then generate a ROC curve for this method by varying the width of the distribution around each ordnance class and declaring each target as ordnance (within the six size bands) or clutter. The result of this analysis is plotted in Figure 16. Also plotted in the Figure is a curve generated by enhancing the magnetometry analysis by taking advantage of the fitted magnetic dipole orientation for each target. This enhancement relies on the observation that UXO targets have, in general, been shock demagnetized by their impact with the ground and only exhibit induced magnetic moments while fragments and clutter have remanent moments. This was the case for the ordnance recovered at the L Range, only one of the 73 items considered had a magnetic dipole orientation not consistent with an induced dipole only. Note that this method does not automatically eliminate all items with a remanent moment, only those whose net dipole orientation is outside that expected from an item with an wholly induced dipole.

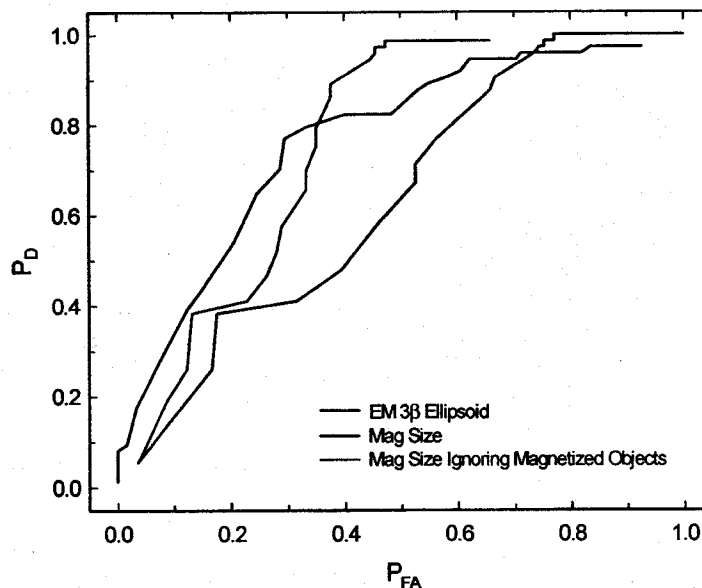


Figure 16 – ROC curve for classification at the L Range comparing the results obtained with the 3-beta algorithm to those using magnetic dipole "size" and dipole orientation enhancements

The magnetic dipole "size" suffers from many of the same problems as the 3-beta algorithm when attempting to discriminate all ordnance. In order to capture the fuzes, a large number of small frag items must be included. The magnetic dipole orientation filter helps greatly in this

regard as a good number of the frag items are magnetized and are thus correctly identified as clutter.

It is difficult to compare the performance of the analysis of EM-61 data presented here with that of other sensors and analysis methods. As we have shown, the current procedure gives excellent results in the test jig and reasonable results at our Test Field, which is a smooth, clean, and level site. The only legitimate comparison is to results obtained by competing technologies on live-site surveys. As these data become available, direct comparisons will follow.

6. Cost Assessment

6.1 Cost Performance

The estimated costs for an *MTADS* EM survey in two directions and the data analysis required to implement the model described here for a hypothetical 200 acre survey are listed in Table IV.

Table IV – Estimated Costs for a Hypothetical 200-Acre Survey Using These Methods.

Mobilization and Logistics		Survey and Analysis		Demobilization	
Activity	\$K	Activity	\$K	Activity	\$K
Planning and Contracting	10	Surface Clearance	30	Site Cleanup	10
Equipment Transport	5	Field Surveys	200	Demobilization	5
Storage and Offices	5	Data Analysis	25		
Power and Fuel	3	Target Flagging	25		
Miscellaneous	2				
Total	25	Total	280	Total	15

Note that the survey costs include two EM surveys only, no magnetometer survey is included. If large, deep targets were expected a magnetometer survey would be required and an additional \$80K would be necessary. Since two perpendicular EM surveys are included in the estimate while only one would be required for target detection, it is clear that the added cost of these methods is \$500 per acre. This is approximately equal to the costs required to remediate three targets per acre. Thus, the economic breakeven point for the use of these methods is reached when three false alarms per acre are avoided.

7. Technology Implementation

7.1 DoD Need

Past DoD activities have contaminated large tracts of land and water with UXO. It is estimated that there are millions of acres of suspect land and there are 600 FUDS and 44 BRAC sites requiring remediation. This UXO contamination prevents civilian use of the land and will thus require remediation. Approximately \$125 M/yr is being spent in the FUDS and BRAC process. Thus, this is a large problem for the DoD and one where R&D efforts can be repaid many times over.

The cost of a current technology UXO remediation operation is driven by false alarms. The Army Corps of Engineers has estimated that during the clean up of a heavily contaminated 5000-acre site, 76% or \$22.8M of the required funds goes to non-UXO removal. Obviously, any techniques that can reduce this false alarm problem should be investigated.

7.2 Transition

The baseline *MTADS* technology has been transitioned via a Cooperative Research and Development Agreement between NRL and Blackhawk Geometrics of Golden CO. Blackhawk has replicated both the magnetometer and EM arrays using the engineering drawings and plans provided to them under a license agreement from NRL. The baseline *MTADS* data analysis system was also transitioned using this agreement. Both Blackhawk and NRL have continued to improve the data analysis system both jointly and independently. For example, both groups are now running the DAS on a LINUX-based PC instead of the older UNIX work stations. Both groups have also worked over the past two years to extract classification information from EM induction survey data. This program is an example of these efforts.

The results of this program have been, and will continue to be, communicated to the UXO community through presentations and publications. There have been several presentations each of the past two years at the UXO Forum and we plan to present a wrap-up talk next year. We have submitted a paper on these methods and the results of the Demonstrations to the upcoming special issue of the *IEEE Transactions on Geoscience and Remote Sensing* on UXO. By these means, we mean to keep the entire community of time-domain EM induction sensor users informed of our progress, not just the users of the commercial *MTADS*.

The fitting methods from this program will be used in part during the Jefferson Proving Ground Demonstration in late Summer 2000. This should provide a good test of these methods at a blind ordnance detection/classification exercise. If they prove successful, we are confident "they will come."

8. References

1. "Hand-held Gradiometer Survey Test at The Marine Corps Air Ground Combat Center, Twentynine Palms, CA," NAVEODTECHCEN TR, September 1992. This report describes hand-held gradiometer surveys of the MCAGCC Magnetic Test Range conducted by military EOD teams. Their ordnance detection efficiency varied between 25 and 35%.
2. "MTADS TECHEVAL Demonstration, October 1996," H. H. Nelson, J. R. McDonald, and Richard Robertson, NRL/PU/6110--97-348.
3. "Results of the MTADS Technology Demonstration #2, Magnetic Test Range, Marine Corps Air Ground Combat Center, Twentynine Palms, CA, December 1996," J. R. McDonald, H. H. Nelson, R. A. Jeffries, and Richard Robertson, NRL/PU/6110--97-349.
4. "Results of the MTADS Technology Demonstration #3, Jefferson Proving Ground, Madison, IN, January 13-24, 1997," H. H. Nelson, J. R. McDonald, R. A. Jeffries, and Richard Robertson, NRL/PU/6110--99-375.
5. "MTADS Unexploded Ordnance Operations at the Badlands Bombing Range, Pine Ridge Reservation, Cury Table, SD, July 1997," J. R. McDonald, H. H. Nelson, J. Neece, Richard Robertson and R. A. Jeffries, NRL/PU/6110--98-353.
6. "MTADS Demonstration at the Former Ft. Pierce Amphibious Base, Vero Beach, FL, March 1998," J. R. McDonald, H. H. Nelson, R. A. Jeffries, Richard Robertson, and K. Blankinship, NRL/PU/6110--98-372.
7. "MTADS Live Site Survey, Bombing Target #2 at The Former Buckley Field, Arapahoe County, CO," J. R. McDonald, H. H. Nelson and R. Robertson NRL/PU/6110--99-379.
8. "MTADS Geophysical Survey at The Jamaica Island and Topeka Pier Landfills at The Portsmouth Naval Shipyard, Kittery, ME, October 1998," J. R. McDonald, H. H. Nelson and B. Puc, NRL/PU/6110--99-381.
9. "MTADS Live Site Demonstration, Pueblo of Laguna, 6 July - 7 August 1998," J. R. McDonald, H. H. Nelson and R. A. Jeffries NRL/PU/6110--00-398.
10. "MTADS UXO Survey and Remediation on the Walker River Paiute Reservation, Schurz, NV, November 1998," J. R. McDonald, H. H. Nelson, and R. A. Jeffries NRL/PU/6110--00-406.
11. "MTADS Geophysical Survey of Potential Underground Storage Tank Sites at the Naval District Washington, Anacostia Annex," H. H. Nelson, J. R. McDonald, R. Robertson, and B. Puc, NRL/MR/6110--00-8435.
12. "Navy Tri-Service Environmental Quality Research Development, Test and Evaluation Strategic Plan," of October 1994, Cleanup p. 21.

13. "Design and Construction of the NRL Baseline Ordnance Classification Test Site at Blossom Point," H. H. Nelson, J. R. McDonald, and R. Robertson, NRL/MR/6110--00-8437.
14. "Collection and Analysis of Multi-sensor Ordnance Signatures with *MTADS*," Bruce Barrow and H. H. Nelson, *J. Environ. Engineering Geophysics*, **3**, 71 (1998).
15. "Model-Based Characterization of EM Induction Signatures for UXO/Clutter Discrimination Using the *MTADS* Platform," Bruce Barrow and H. H. Nelson, Proceedings of the UXO Forum 1999, Atlanta GA, May 25-27, 1999.
16. "Model-Based Characterization of EM Induction Signatures Obtained with the *MTADS* EM Array," Bruce Barrow and H. H. Nelson, *IEEE Trans. Geophys. Remote Sens.*, submitted
17. "Draft Final Removal Report: Ordnance Removal at Army Research Laboratory, Blossom Point Field Test Facility (BPFTF), Blossom Point, Maryland," Human Factors Applications, Inc., DACA87-95-D-0027, Task Order 0008, 18 April 1997.

Appendix A. Points of Contact

ESTCP

Dr. Jeffrey Marqusee	ESTCP Director	Tel: 703-696-2120 Fax: 703-696-2114 marqusj@acq.osd.mil
----------------------	----------------	---

Ms. Catherine Vogel	Program Manager, Cleanup	Tel: 703-696-2118 Fax: 703-696-2114 vogelc@acq.osd.mil
---------------------	--------------------------	--

Institute for Defense Analyses

Dr. Anne Andrews	Analyst	Tel: 703-578-2966 Fax: 703-578-2877 AAndrews@ida.org
------------------	---------	--

NRL

Dr. Herbert Nelson	Principal Investigator	Tel: 202-767-3686 Fax: 202-404-8119 herb.nelson@nrl.navy.mil
--------------------	------------------------	--

Dr. J. R. McDonald	Deputy Principal Investigator	Tel: 202-767-3340 Fax: 202-404-8119 j.mcdonald@nrl.navy.mil
--------------------	-------------------------------	---

Army Research Laboratory, Blossom Point

Mr. Jack Kaiser	Site Manager	Tel: 301-870-2329 Fax: 301-870-3130 jkaiser@arl.mil
-----------------	--------------	---

Mr. Bill Davis	Explosives Safety Officer	Tel: 301-394-2434 Fax: 301-394-2514 wdavis@arl.mil
----------------	---------------------------	--

Hughes Associates, Inc.

Mr. Richard Robertson	Program Manager	Tel: 202-767-3556 Fax: 202-404-8119 roberts5@ccf.nrl.navy.mil
-----------------------	-----------------	---

GeoCenters, Inc.

Mr. Larry Koppe

Site Safety Officer

**Tel: 301-753-1690
Fax: 301-870-3130
LarryEOD@aol.com**

AETC, Inc.

Dr. Tom Bell

Project Manager

**Tel: 703-413-0500
Fax: 703-413-0505
tbell@va.aetc.com**

Dr. Bruce Barrow

Project Scientist

**Tel: 703-413-0500
Fax: 703-413-0505
bjb@va.aetc.com**

Appendix B. Data Archiving and Demonstration Plan

MTADS survey data are collected as a collection of data files each containing the time-stamped (DAQ computer time) input stream from the individual sensors. These input streams include GPS UTC time, GPS pulse-per-second (PPS), GPS position, sensor trigger, and sensor input data. After transfer of the files to the *MTADS* DAS, the data undergo a preprocessing step in which all times are corrected to UTC and the individual sensor positions are interpolated from the measured positions vs. time in the GPS position file. Magnetometer data are then corrected by removing the diurnal variation of the Earth's field as measured by a reference sensor located near the survey site and the heading error resulting from residual vehicle signature. EM data have the long term baseline drift of the sensors removed by subtracting a 1000-point running median from the data. At this point, the survey data are available as background-corrected, geo-referenced, mapped data files.

Both the raw input data files and an ASCII version of the mapped data file are archived. The preprocessed data file is most useful for other investigators and these files are maintained on a CD-ROM by the principal investigator. These data files and a copy of the approved test plan are available by contacting Herb Nelson at herb.nelson@nrl.navy.mil.

This page left blank intentionally.

Appendix C. MTADS Target Report from the Final Demonstration

Target #	Mag Local X (m)	Mag Local Y (m)	Mag Depth (m)	3β Local X (m)	3β Local Y (m)	3β EM Depth (m)	Mag Size (m)	Mag Moment	Fit Quality	β1	β2	β3	Theta	Phi	Psi	χ2	3β Coherence	Remediation Results
FUS-1	184.40	106.05	0.09	184.34	106.05	0.08	0.037	0.027	0.972	0.73	0.04	0.05	0.00	0.00	0.00	137.0	0.967	Frag
FUS-2	175.73	125.13	0.07	175.57	125.29	0.03	0.035	0.023	0.981	0.39	0.04	0.11	-69	-136	18	808.1	0.969	Frag
FUS-3	164.98	135.15	0.10	164.92	135.18	0.11	0.068	0.515	0.950	1.84	0.31	0.60	-10	123	-41	1349.4	0.968	Frag
FUS-4	158.60	135.47	0.38	158.63	135.40	0.36	0.134	0.212	0.981	10.41	0.77	0.39	0.00	0.00	0.00	382.10	0.981	Frag
FUS-5	170.89	134.25	0.16	170.85	134.38	0.12	0.040	0.035	0.965	1.93	0.54	0.30	11	-168	-117	1308.6	0.965	Non-Ordnance
FUS-6	158.13	145.54	0.45	158.42	145.46	0.37	0.083	0.311	0.943	4.99	1.64	1.86	-31	151	-165	1081.8	0.971	81-mm Mortar
FUS-7	153.48	141.09	0.24	153.76	141.09	0.11	0.070	0.189	0.943	0.55	0.45	0.39	30	135	132	681.0	0.943	Ordinance Related
FUS-8	151.64	180.20	0.09	151.7	180.13	0.19	0.026	0.010	0.902	1.79	0.35	0.66	32	107	-34	1268.9	0.964	Frag
FUS-9	138.88	202.80	0.17	138.97	202.79	0.06	0.092	0.427	0.959	0.25	0.17	0.23	-1	-40	-166	305.2	0.950	Non-Ordnance
FUS-10	143.15	120.06	0.12	143.28	120.16	0.14	0.036	0.026	0.962	0.96	0.33	0.62	0.00	0.00	0.00	133.6	0.962	Ordinance Related
FUS-11	138.90	163.80	0.08	138.86	163.78	-0.02	0.080	0.279	0.992	0.13	0.03	0.06	-4	-121	-89	70.8	0.949	Frag
FUS-12	142.93	153.88	0.18	143.34	153.86	0.19	0.072	0.206	0.914	0.93	0.17	0.58	-8	26	82	435.8	0.852	Frag
FUS-13	146.3	194.07	0.01	146.3	194.5	0.13	0.032	0.013	0.980	0.8	0.02	0.05	0.00	0.00	0.00	345.3	0.980	Frag
FUS-14	130.02	163.44	0.50	129.91	163.41	0.48	0.077	0.250	0.967	3.37	1.71	1.55	-63	69	146	504.6	0.972	81-mm Mortar
FUS-15	128.37	154.60	0.07	128.18	155.19	0.09	0.085	0.470	0.993	0.95	0.60	0.29	5	-84	11	967.3	0.940	Frag
FUS-16	132.61	150.66	0.08	132.72	151.07	0.08	0.083	0.311	0.992	0.73	0.02	0.07	0.00	0.00	0.00	787.4	0.992	Frag
FUS-17	123.03	132.85	0.10	123.06	132.89	0.02	0.047	0.055	0.898	0.73	0.02	0.07	-24	88	-155	787.4	0.968	Frag
FUS-18	123.87	189.98	0.10	123.77	190.09	0.02	0.031	0.016	0.964	0.32	0.02	0.00	58	-71	-5	355.5	0.965	Frag
FUS-19	124.10	112.56	0.05	124.01	112.57	0.03	0.049	0.062	0.992	0.62	0.03	0.00	0.00	0.00	0.00	418.2	0.992	Non-Ordnance
FUS-20	116.29	155.73	0.63	116.58	155.89	0.33	0.288	13.033	0.925	12.13	7.03	3.92	-2	62	40	7002.8	0.953	Non-Ordnance
FUS-21	119.36	159.32	0.12	119.3	159.28	0.06	0.035	0.024	0.811	0.67	0.46	0.33	46	-9	83	738.6	0.975	Cone-shaped Warhead
FUS-22	114.86	162.38	0.07	114.87	162.38	0.02	0.029	0.013	0.970	0.71	0.02	0.05	10	-20	127	83.3	0.919	Frag
FUS-23	112.19	168.08	0.53	112.18	168.07	0.21	0.342	21.740	0.953	4.41	2.53	1.25	-12	-152	-72	1719.8	0.985	Non-Ordnance
FUS-24	113.05	171.41	0.13	113.12	171.41	0.14	0.044	0.047	0.892	1.67	0.25	0.96	-2	-155	-100	1337.1	0.917	Non-Ordnance
FUS-25	99.69	158.16	0.32	99.8	158.16	0.32	0.032	0.013	0.970	0.71	0.02	0.05	10	-20	127	83.3	0.919	Non-Ordnance
FUS-26	89.48	141.77	0.09	89.55	141.83	0.03	0.033	0.019	0.858	0.45	0.37	0.33	-8	169	-45	477.1	0.982	Ordinance Related
FUS-27	96.67	144.71	0.55	96.97	144.46	0.52	0.082	0.303	0.989	9.02	3.00	5.18	-37	80	-114	1126.0	0.961	Projectile with Frag Sleeve
FUS-28	101.09	148.81	0.49	101.99	148.81	0.19	0.033	0.013	0.939	0.34	0.04	0.45	0.00	0.00	0.00	95.16	0.939	Frag
FUS-29	91.48	122.56	0.11	91.5	122.66	0.03	0.037	0.027	0.887	0.30	0.19	0.26	42	20	124	367.5	0.972	Ordinance Related
FUS-30	104.61	109.57	0.16	104.71	109.49	0.13	0.058	0.107	0.906	1.08	0.84	0.70	-10	-37	-13	1398.7	0.964	Ordinance Related
FUS-31	102.79	105.80	0.16	102.7	105.76	0.07	0.060	0.118	0.837	5.08	1.65	1.26	5	30	169	322.5	0.980	76mm Mortar
FUS-32	94.74	102.22	0.66	94.5	102.34	0.36	0.091	0.414	0.981	2.90	1.79	1.25	40	154	-26	590.2	0.969	81-mm Mortar
FUS-33	79.25	96.98	0.13	79.2	97.04	0.08	0.041	0.038	0.939	1.32	0.15	0.19	-2	-77	159	265.7	0.975	Ordinance Related
FUS-34	82.35	109.49	0.11	81.71	109.59	0.07	0.051	0.106	0.988	0.8	0.10	0.05	0.00	0.00	0.00	265.6	0.928	Frag

Target #	Mag Local X (m)	Mag Local Y (m)	Mag Depth (m)	3β Local X (m)	3β Local Y (m)	3β EM Depth (m)	Mag Size (m)	Mag Moment	Fit Quality	β1	β2	β3	Theta	Phi	Psi	χ2	3β Coherence	Remediation Results
FUS-35	78.17	141.27	0.13	77.98	141.26	0.14	0.041	0.036	0.920	0.77	0.54	0.10	-10	95	172	341.9	0.929	Frag
FUS-36	76.38	139.16	0.26	76.39	138.96	0.24	0.048	0.060	0.791	1.06	0.24	0.52	-12	-65	-85	250.3	0.928	Frag
FUS-37	79.93	138.19	0.13	79.55	138.37	0.26	0.033	0.019	0.769	0.53	0.41	0.10	10	75	83	444.5	0.930	Frag
FUS-38	80.56	141.07	0.41	80.7	141.04	0.22	0.036	0.026	0.829	0.86	0.52	0.17	-16	35	29	197.9	0.956	Frag
FUS-39	76.19	165.19	0.17	76.12	165.24	0.11	0.046	0.052	0.972	1.23	0.23	0.18	6	100	163	517.7	0.962	Frag
FUS-40	81.68	165.59	0.03	81.73	165.57	0.12	0.089	0.388	0.933	0.80	0.41	0.19	15	75	83	444.5	0.959	Frag
FUS-41	84.51	169.42	0.50	84.51	169.32	0.34	0.264	9.999	0.946	4.97	0.83	1.47	25	-127	-180	806.3	0.950	Non-Ordnance
FUS-42	77.58	179.65	0.54	77.75	179.5	0.39	0.086	0.340	0.963	3.13	1.11	1.67	31	6	166	1248.8	0.950	81-mm Mortar
FUS-43	75.70	178.83	0.12	75.45	179.16	0.29	0.037	0.029	0.857	1.38	0.25	0.43	7	55	14	359.5	0.915	Non-Ordnance
FUS-44	83.78	181.19	0.45	83.46	181.3	0.40	0.094	0.457	0.939	7.25	1.78	2.56	21	147	57	866.6	0.968	81-mm Mortar
FUS-45	77.82	183.79	0.06	77.81	183.76	0.04	0.071	0.197	0.929	0.32	0.01	0.00	5	-62	-116	115.7	0.935	Frag
FUS-46	59.75	173.51	0.13	59.5	173.75	0.53	0.095	0.107	0.948	7.11	2.55	1.77	54	73	6	249.7	0.980	81-mm Mortar
FUS-47	73.18	153.65	0.24	73.19	153.72	0.12	0.164	2.411	0.965	2.73	1.17	0.39	72	-44	-112	2600.3	0.982	Non-Ordnance
FUS-48	64.93	139.90	0.08	64.87	139.98	0.18	0.032	0.017	0.780	1.52	0.00	0.07	3	-180	-151	419.8	0.938	Frag
FUS-49	73.37	120.47	0.07	73.65	120.47	0.16	0.01	0.01	0.988	0.51	0.11	0.11	14	112	156	381.9	0.937	Non-Ordnance
FUS-50	67.23	118.92	0.08	67.31	118.89	0.08	0.102	0.574	0.987	0.74	0.05	0.06	14	112	156	381.9	0.937	No Dig Sheet
FUS-51	69.50	94.68	0.06	69.42	94.63	0.08	0.052	0.078	0.989	3.23	0.85	0.42	-1	177	-174	9141.3	0.925	Non-Ordnance
FUS-52	48.17	131.23	0.08	47.99	131.25	0.04	0.027	0.013	0.921	0.36	0.29	0.22	26	123	22	222.5	0.954	Frag
FUS-53	46.30	133.26	0.07	46.12	133.16	0.09	0.043	0.043	0.916	1.94	0.45	0.62	14	172	-87	2197.4	0.968	Frag
FUS-54	59.48	152.90	0.05	59.47	152.86	0.11	0.071	0.198	0.977	1.00	0.00	0.07	-1	107	177	452.4	0.921	Non-Ordnance
FUS-55	52.37	164.19	0.74	52.36	164.14	0.16	0.401	35.101	0.944	9.61	3.56	2.43	21	146	-122	4393.6	0.978	Non-Ordnance
FUS-56	59.91	163.11	0.10	59.9	163.17	0.09	0.026	0.009	0.937	0.59	0.14	0.39	-7	-2	-49	198.8	0.979	Frag
FUS-57	57.82	168.13	0.57	57.84	168.07	0.50	0.091	0.415	0.977	4.91	2.82	2.23	61	-55	77	607.6	0.978	81-mm Mortar
FUS-58	46.54	167.83	0.47	46.49	167.62	0.45	0.104	0.618	0.984	1.97	1.22	0.73	59	160	32	170.8	0.960	Non-Ordnance
FUS-59	55.48	173.89	0.49	55.47	173.73	0.52	0.076	0.243	0.923	4.06	1.80	2.20	62	44	-90	218.5	0.971	81-mm Mortar
FUS-60	37.47	170.69	0.56	37.37	170.89	0.69	0.076	0.238	0.912	6.00	2.17	3.38	-59	-37	-108	218.2	0.978	81-mm Mortar
FUS-61	36.59	159.17	0.19	36.5	159.17	0.12	0.103	0.513	0.985	2.41	0.41	0.41	79	-52	3	230.7	0.983	Frag
FUS-62	43.8	164.26	0.32	43.8	164.26	0.02			0.983	0.21	0.00	0.02	79	-52	3	230.7	0.983	Nothing Found
FUS-63	51.45	40.57	0.45	51.45	40.63	0.38	0.077	0.243	0.980	5.27	1.12	0.59	33	84	-2	784.4	0.957	81-mm Mortar SEED?
FUS-64	77.37	58.42	0.79	76.96	58.67	0.51	0.118	0.886	0.947	11.95	3.27	3.27	8	143	177	1592.0	0.954	4.2" SEED
FUS-65	86.33	56.00	0.31	86.33	56.01	0.29	0.101	0.559	0.932	6.62	0.96	1.49	57	115	10	2315.9	0.987	25lb Frag Bomb
FUS-66	86.19	52.41	0.30	86.1	52.46	0.26	0.047	0.058	0.980	2.86	0.26	0.94	3	15	-161	824.8	0.963	2.75" WH SEED
FUS-67	105.39	62.43	0.29	105.53	62.32	0.19	0.079	0.289	0.982	1.78	0.91	0.61	72	138	118	2721.6	0.964	2.75" WH SEED
FUS-68	111.13	62.61	0.62	111.08	62.58	0.53	0.066	0.155	0.941	9.42	1.34	1.16	9	48	-101	431.7	0.927	81-mm Mortar SEED
FUS-69	124.20	67.11	0.18	124.08	67.16	0.16	0.063	0.133	0.983	4.92	0.63	0.46	-41	32	-71	42666	0.821	MK23 SEED
FUS-70	129.70	73.13	0.10	129.5	73.19	0.04	0.033	0.025	0.967	0.43	0.43	0.41	-11	121	90	720.7	0.972	2.75" RktMort/FlareOpen
FUS-71	68.85	71.70	0.14	68.89	71.66	0.10	0.066	0.155	0.944	3.92	1.43	1.85	-12	-163	-108	2747.3	0.978	81-mm Mortar

Target #	Mag Local X (m)	Mag Local Y (m)	Mag Depth (m)	3β Local X (m)	3β Local Y (m)	3β EM Depth (m)	Mag Size (m)	Mag Moment	Fit Quality	β1	β2	β3	Theta	Phi	Psi	χ2	3β Coherence	Remediation Results
FUS-72	182.05	103.38	0.26	182.14	103	0.37	0.083	0.307	0.811	11.79	2.38	3.67	32	-100	-13	8879.9	0.964	81-mm Mortar
FUS-73	168.12	114.95	0.07	167.77	114.92	0.95	0.031	0.409	0.912	0.75	1.43	3.22	35	100	13	352.2	0.983	Frag
FUS-74	168.27	145.56	0.10	168.68	145.74	0.26	0.074	0.219	0.970	2.06	1.44	0.95	-6	176	154	1537.9	0.920	No Dig Sheet
FUS-75	151.38	155.44	0.11	151.41	155.67	0.14	0.037	0.028	0.957	0.69	0.49	0.53	-6	-180	10	1028.7	0.942	BOMB FUZE
FUS-76	153.89	143.46	0.32	153.62	143.34	0.38	0.056	0.097	0.866	3.33	1.36	1.49	11	36	176	276.0	0.950	Ordnance Related
FUS-77	153.21	158.10	0.30	153.29	157.32	0.19	0.087	0.363	0.945	1.26	0.19	0.50	13	-148	-141	307.1	0.970	Frag
FUS-78	133.95	187.04	0.44	133.95	187.04	0.14			0.986	8.95	2.97	4.95	10	26	79	7499.0	0.986	Non-Ordnance
FUS-79	133.94	191.98	0.37	133.63	191.89	0.44	0.073	0.213	0.956	5.64	1.78	2.82	10	166	114	1741.3	0.957	81-mm Mortar
FUS-80	133.99	183	0.66	133.99	183	0.36			0.946	6.93	2.92	1.94	-21	-5	-152	2692.6	0.946	Non-Ordnance
FUS-81	129.53	190.78	0.08	129.33	190.8	0.08	0.080	0.280	0.969	0.34	0.26	0.06	-20	119	166	197.4	0.939	Frag
FUS-82	132.17	135.05	0.13	132.17	135.05	0.09			0.937	0.24	0.09	0.09	32	100	120	143.0	0.957	Nothing Found
FUS-83	168.47	99.63	0.14	168.5	99.89	0.09	0.078	0.258	0.955	4.93	1.11	1.29	2	-113	-175	15748	0.953	MORTAR?
FUS-84	166.78	106.86	0.13	166.87	106.96	0.09	0.059	0.109	0.972	0.69	0.11	0.18	-82	158	4	868.2	0.981	Non-Ordnance
FUS-85	164.90	107.62	0.11	164.8	107.81	0.37	0.112	0.255	0.915	6.12	2.01	3.05	15	30	106	350.1	0.915	81mm Mortar
FUS-86	165.32	120.7	0.56	165.32	120.7	0.26			0.944	1.46	0.41	1.04	-25	113	-76	562.9	0.944	Frag
FUS-87	165.3	124.12	0.42	165.3	124.12	0.12			0.967	1.05	0.13	0.70	-24	124	170	1616.5	0.967	Frag
FUS-88	149.67	111.73	0.33	149.67	111.73	0.08			0.952	0.62	0.11	0.15	7	24	88	2936.7	0.952	Ordnance Related
FUS-89	158.99	113.81	0.13	158.71	113.94	0.23	0.037	0.027	0.930	2.20	0.88	1.80	6	173	121	1199.2	0.963	Ordnance Related
FUS-90	157.74	117.69	0.21	158.11	117.53	0.37	0.042	0.040	0.902	2.26	2.04	0.45	20	-31	-24	1220.7	0.888	Frag
FUS-91	160.94	118.81	0.08	160.92	118.92	0.28	0.036	0.025	0.869	2.30	1.10	0.91	17	171	83	2897.7	0.872	Ordnance Related
FUS-92	161.53	116.61	0.16	161.61	116.61	0.20	0.055	0.091	0.981	6.22	3.04	2.29	-5	-2	-5	6318.0	0.972	81-mm Mortar
FUS-93	149.21	158.38	0.14	149.24	158.33	0.09	0.041	0.036	0.888	0.93	0.22	0.16	-15	13	-44	699.1	0.957	Frag
FUS-94	159.92	164.63	0.02	160.07	164.67	0.05	0.095	0.467	0.932	1.14	0.4	0.44	9	135	137	1684.7	0.968	Frag
FUS-95	136.68	96.36	0.15	136.75	96.5	0.08	0.041	0.037	0.967	0.71	0.34	0.18	16	99	-137	848.1	0.920	2.75"RktMtr
FUS-96	136.14	101.52	0.08	136.07	101.48	0.17	0.059	0.112	0.915	5.67	3.00	2.67	-10	28	-124	7030.2	0.981	Recoilless Rifle Round 76-80mm/18"
FUS-97	137.75	149.22	0.13	137.83	149.16	0.17	0.052	0.075	0.940	2.70	1.28	0.66	12	100	173	4270.5	0.938	Ordnance Related
FUS-98	138.74	147.83	0.25	138.5	147.65	0.39	0.148	1.747	0.960	4.83	0.25	0.35	6	95	113	599.5	0.924	Frag
FUS-99	137.71	146.32	0.19	137.4	146.24	0.09	0.043	0.044	0.747	0.65	0.22	0.05	-62	-52	108	1862.2	0.958	Frag
FUS-100	138.32	143.45	0.32	138.55	143.38	0.27	0.045	0.049	0.619	1.69	0.38	1.02	33	17	77	648.4	0.938	Ordnance Related
FUS-101	140.33	175.30	0.07	140.3	175.27	0.13	0.090	0.397	0.997	0.47	0.02	0.12	5	-165	110	155.9	0.888	Frag
FUS-102	133.83	171.49	0.09	134.22	172.19	0.23	0.059	0.113	0.933	1.14	0.56	1.10	11	85	-100	500.0	0.945	Frag
FUS-103	137.26	191.62	0.19	137.26	191.87	0.19	0.035	0.052	0.985	1.30	1.5	0.52	20	81	168	2619.2	0.975	Non-Ordnance
FUS-104	138.56	191.62	0.20	138.33	191.7	0.24	0.036	0.026	0.948	2.51	0.93	1.42	-13	-3	170	2155.4	0.966	60mmMortar
FUS-105	136.68	189.81	0.26	136.7	189.87	0.24	0.062	0.132	0.960	5.65	1.53	1.13	18	36	41	2210.2	0.986	81-mm Mortar
FUS-106	132.8	155.46	0.18	132.97	155.37	0.21	0.190	0.330	0.892	1.35	0.41	0.60	12	100	173	4270.5	0.938	Frag
FUS-107	126.83	94.48	0.54	126.76	94.45	0.45	0.243	7.832	0.859	189.02	45.23	89.93	2	-178	-77	815158	0.918	5"Rkt
FUS-108	124.10	96.01	0.13	124.14	96.06	0.04	0.032	0.017	0.761	5.30	1.40	3.62	-45	119	127	71941	0.972	Non-Ordnance

Target #	Mag Local X (m)	Mag Local Y (m)	Mag Depth (m)	3β Local X (m)	3β Local Y (m)	3β EM Depth (m)	Mag Size (m)	Mag Moment	Fit Quality	β1	β2	β3	Theta	Phi	Psi	χ2	3β Coherence	Remediation Results
FUS-109	130.87	112.16	0.40	131.36	112.58	0.07	0.110	0.728	0.693	1.47	1.98	2.02	-4	86	-47	2118.2	0.963	Frag
FUS-110	123.26	123.52	0.11	123.32	123.36	-0.01	0.041	0.036	0.940	0.25	0.15	0.20	9	-104	-123	451.4	0.950	Ordinance Related
FUS-111	129.01	123.99	0.21	128.91	124.09	0.16	0.072	0.200	0.922	0.92	0.20	0.73	5	130	-85	537.7	0.916	Frag
FUS-112	125.64	136.44	0.26	125.55	136.46	0.26	0.037	0.028	0.861	2.16	1.63	1.16	-55	-101	-122	1381.3	0.980	81-mm Mortar
FUS-113	128.76	136.30	0.11	128.69	136.25	0.10	0.042	0.041	0.925	0.47	0.34	0.26	-6	-10	-152	253.5	0.973	Non-Ordinance
FUS-114	123.54	162.86	0.22	123.5	162.74	0.17	0.103	0.585	0.936	4.18	0.65	0.56	1	72	-180	1404.7	0.966	Non-Ordinance
FUS-115	130.77	175.58	0.35	130.61	175.46	0.37	0.080	0.270	0.980	5.81	2.51	2.41	163	-177	-163	1637.6	0.980	No-Dig Sheel
FUS-116	122.95	175.89	0.08	122.84	175.9	0.27	0.040	0.035	0.986	3.75	0.57	0.31	2	-95	-9	1539.8	0.897	Non-Ordinance
FUS-117	119.33	166.90	0.44	119.51	166.9	0.37	0.087	0.352	0.958	7.60	2.00	3.20	33	-24	-143	6522.1	0.955	81-mm Mortar
FUS-118	123.23	168.45	0.11	122.88	168.7	0.12	0.015	0.012	0.707	0.6	0.7	0.20	21	-101	-59	1022.1	0.941	Frag
FUS-119	126.29	197.71	0.05	126.35	197.51	0.06	0.041	0.038	0.888	0.92	0.27	0.29	7	2	-46	427.6	0.965	Ordinance Related
FUS-120	133.84	204.27	0.09	133.88	204.32	0.11	0.051	0.074	0.968	0.58	0.38	0.28	41	165	120	398.5	0.970	Ordinance Related
FUS-121	113.27	78.31	0.17	113.62	78.29	0.27	0.061	0.122	0.877	1.77	0.33	0.20	1	-183	-12	340.4	0.905	Non-Ordinance
FUS-122	108.73	88.75	0.18	108.77	88.79	0.15	0.064	0.142	0.894	5.02	2.01	2.10	-3	57	-171	6490.4	0.979	81-mm Mortar
FUS-123	111.67	100.19	0.11	111.51	100.22	0.13	0.087	0.355	0.902	0.84	0.28	0.48	-6	85	114	851.3	0.900	Frag
FUS-124	118.45	106.53	0.55	118.57	106.59	0.42	0.082	0.300	0.957	3.62	1.52	2.10	54	-46	-44	593.6	0.981	81-mm Mortar
FUS-125	120.26	112.66	0.12	120.33	112.83	0.26	0.042	0.039	0.932	1.66	0.68	1.05	-7	-99	102	841.9	0.901	Ordinance Related
FUS-126	113.56	132.65	0.10	113.2	133.16	0.06	0.041	0.037	0.967	0.75	0.25	0.07	-73	43	-145	1025.2	0.976	Frag
FUS-127	108.36	134.57	0.11	108.34	134.66	0.22	0.084	0.321	0.702	1.04	0.05	0.05	3	50	-38	387.5	0.868	Frag
FUS-128	120.67	135.58	0.11	120.66	135.43	0.34	0.064	0.143	0.910	3.05	0.04	0.16	-5	-110	1	802.8	0.859	Non-Ordinance
FUS-129	109.89	153.80	0.47	109.86	153.77	0.12	0.272	10.942	0.897	3.46	1.89	0.71	9	-121	101	4377.4	0.973	Non-Ordinance
FUS-130	111.49	163.56	0.27	111.52	163.55	0.18	0.007	0.013	0.863	0.8	0.87	1.35	2	-10	-30	2929	0.915	81-mm Mortar
FUS-131	108.55	164.24	0.37	108.68	164.37	0.42	0.060	0.120	0.660	4.09	1.76	2.99	-44	126	-60	319.0	0.985	81-mm Mortar
FUS-132	115.74	167.11	0.09	115.69	167.02	0.09	0.061	0.122	0.983	3.66	0.78	2.16	-5	-2	-107	5265.1	0.971	Non-Ordinance
FUS-133	89.84	190.89	0.10	89.77	190.91	0.13	0.082	0.259	0.985	1.26	0.61	0.41	5	-74	0	776.5	0.954	80mm Mortar
FUS-134	88.15	184.29	0.06	88.15	184.31	-0.04	0.085	0.331	0.981	0.14	0.00	0.01	-7	-18	-38	51.9	0.926	Frag
FUS-135	91.05	177.83	0.04	91.11	177.85	0.06	0.049	0.063	0.984	1.46	0.70	0.27	8	-91	-17	660.7	0.978	Frag
FUS-136	91.11	175.62	0.12	90.88	175.14	0.06	0.071	0.198	0.957	0.28	0.10	0.23	27	-60	-127	281.1	0.959	Frag
FUS-137	93.82	174.63	0.59	93.88	174.45	0.27	0.337	20.752	0.956	4.66	1.31	2.46	34	-118	25	3925.3	0.961	Non-Ordinance
FUS-138	94.64	172.09	0.01	94.71	172.17	0.11	0.042	0.039	0.783	2.48	1.87	1.43	8	-87	-23	3358.2	0.968	81mm Nose Section
FUS-139	96.03	178.16	0.24	95.25	177.11	0.30	0.095	0.235	0.703	1.31	0.11	0.26	5	-10	-10	2367.7	0.915	Frag
FUS-140	101.05	171.69	0.25	100.98	171.81	0.22	0.154	1.983	0.988	17.28	9.43	13.14	-45	-24	-118	135963.	0.968	Frag
FUS-141	94.33	158.52	0.13	94.35	158.42	0.17	0.075	0.227	0.981	0.93	0.35	0.22	44	-58	-1	1256.7	0.946	Frag
FUS-142	90.06	157.56	0.36	90.06	157.5	0.35	0.355	21.751	0.979	1.7	2.65	1.87	10	-10	-10	1022.5	0.970	Non-Ordinance
FUS-143	86.70	157.14	0.30	86.81	157.39	0.30	0.084	0.317	0.986	6.46	1.98	0.91	-42	-124	138	1979.0	0.985	81-mm Mortar
FUS-144	92.85	157.30	0.11	92.71	156.53	0.02	0.064	0.143	0.817	0.47	0.02	0.07	47	-88	148	1563.3	0.948	Frag
FUS-145	96.22	151.97	0.53	96.08	152.07	0.30	0.329	9.850	0.877	10.73	2.71	3.75	10	-36	-186	8283.4	0.970	Non-Ordinance

Target #	Mag Local X (m)	Mag Local Y (m)	Mag Depth (m)	3β Local X (m)	3β Local Y (m)	3β EM Depth (m)	Mag Size (m)	Mag Moment	Fit Quality	β1	β2	β3	Theta	Phi	Psi	χ2	3β Coherence	Remediation Results
FUS-146	94.98	119.88	0.42	94.88	119.51	0.63	0.058	0.104	0.893	14.51	3.98	1.43	30	-86	34	3184.2	0.929	81-mm Mortar
FUS-147	96.13	122.24	0.09	96.07	122.16	0.15	0.050	0.066	0.836	2.94	1.20	2.03	12	-59	-68	5986.2	0.911	BombFuze
FUS-148	91.29	117.57	0.75	90.92	117.91	0.98	0.130	1.187	0.968	48.84	14.22	8.10	27	-115	-133	1096.4	0.948	105mm Plus Scrap
FUS-149	95.12	115.82	0.20	94.66	115.95	0.14	0.049	0.066	0.800	0.73	0.14	0.33	63	-172	-68	996.4	0.963	Frag
FUS-150	97.11	109.69	0.29	97.11	109.74	0.34	0.075	0.228	0.875	3.89	2.26	3.27	16	121	109	2661.4	0.943	4.2" Broke in Half
FUS-151	97.63	94.70	0.92	97.54	94.72	0.07	0.057	0.098	0.850	4.45	1.42	1.69	10	-62	-26	974.1	0.967	Frag
FUS-152	105.68	90.28	0.08	105.17	90.29	0.05	0.108	0.688	0.974	1.25	0.84	1.00	69	-7	-48	3833.6	0.971	Frag
FUS-153	92.88	72.93	0.22	92.89	72.68	0.29	0.078	0.257	0.829	3.76	2.15	2.03	30	12	66	1540.5	0.978	81-mm Mortar
FUS-154	78.77	71.03	0.10	78.85	71.06	0.11	0.074	0.224	0.897	8.10	2.91	1.66	3	-17	-53	2158.6	0.981	81mm Mldm
FUS-155	81.02	76.06	0.19	81.05	76.19	0.19	0.083	0.315	0.943	4.66	2.28	1.41	42	33	170	11688.7	0.958	81-mm Mortar
FUS-156	74.53	70.36	0.21	74.59	70.29	0.23	0.062	0.132	0.953	6.79	3.69	2.35	4	167	16	15916.3	0.925	81-mm Mortar
FUS-157	76.19	72.49	0.09	76.15	72.55	0.12	0.045	0.145	0.962	3.41	1.15	0.90	1	-37	-61	161.5	0.910	Frag
FUS-158	84.51	86.96	0.17	84.59	86.91	0.13	0.032	0.018	0.964	2.01	0.51	0.86	-3	141	-91	1186.9	0.969	Frag
FUS-159	82.38	118.97	0.48	82.28	118.92	0.42	0.085	0.333	0.948	3.71	2.02	2.44	-52	9	92	654.3	0.983	81-mm Mortar
FUS-160	79.13	114.53	0.45	78.86	114.35	0.47	0.070	0.186	0.966	5.17	1.93	2.60	43	-92	-93	1499.7	0.962	81-mm Mortar
FUS-161	83.50	142.28	0.56	83.71	142.17	0.43	0.085	0.330	0.967	7.97	2.09	3.22	27	-12	58	2417.7	0.954	81-mm Mortar
FUS-162	77.86	167.73	0.35	77.86	167.73	0.05			0.977	0.28	0.19	0.25	35	-128	160	164.6	0.977	Ordnance Related
FUS-163	75.97	173.65	0.12	75.93	173.86	0.66	0.045	0.049	0.827	0.86	0.54	0.70	15	-56	-41	803.1	0.976	Ordnance Related
FUS-164	83.62	173.63	0.78	83.95	173.19	0.86	0.332	19.820	0.886	41.23	0.00	40.33	-42	-116	44	10115.4	0.926	Non-Ordnance
FUS-165	74.88	182.53	0.64	74.73	182.7	0.41	0.073	0.212	0.905	3.91	0.53	1.62	8	-111	-10	1346.3	0.907	81-mm Mortar
FUS-166	74.38	187.01	0.45	74.48	187.21	0.69	0.088	0.203	0.931	3.15	1.69	1.21	9	-55	-53	233.9	0.981	81-mm Mortar
FUS-167	81.47	186.46	0.42	81.82	186.88	0.65	0.055	0.092	0.947	10.54	3.16	1.69	9	49	-58	695.7	0.915	81-mm Mortar
FUS-168	83.42	188.39	0.55	83.52	188.68	0.84	0.293	13.672	0.941	28.63	2.85	0.00	54	45	122	11281.8	0.889	Non-Ordnance
FUS-169	63.84	185.26	0.58	63.88	185.31	0.47	0.072	0.259	0.973	2.61	1.98	0.77	39	-55	-58	240.5	0.981	81-mm Mortar
FUS-170	64.40	183.25	0.38	64.39	183.12	0.42	0.067	0.165	0.950	7.23	2.62	2.11	26	-74	49	1755.0	0.970	81-mm Mortar
FUS-171	66.42	182.07	0.51	66.75	182.18	0.75	0.073	0.215	0.981	4.80	0.78	1.53	35	151	114	314.0	0.969	81-mm Mortar
FUS-172	58.50	170.57	0.25	60.68	170.68	0.58	0.244	7.842	0.772	8.29	3.11	2.43	30	175	148	592.3	0.967	Frag
FUS-173	62.97	170.42	0.09	62.96	170.35	0.11	0.124	1.026	0.731	3.94	1.13	0.54	-6	-127	155	1957.3	0.978	Frag
FUS-174	67.74	168.10	0.48	67.6	167.98	0.37	0.112	0.769	0.950	8.08	2.41	4.88	36	-117	-164	2574.6	0.983	81-mm Mortar
FUS-175	65.69	157.17	0.04	65.65	157.21	0.11	0.036	0.025	0.792	0.97	0.73	0.55	12	99	174	1076.1	0.966	Frag
FUS-176	71.00	159.89	0.33	71.37	159.62	0.47	0.070	0.185	0.962	5.60	2.19	1.69	30	-51	-137	823.1	0.976	Frag
FUS-177	60.18	151.02	0.01	60.19	151	0.02	0.039	0.033	0.994	0.74	0.11	0.07	-3	-149	-177	752.4	0.945	Non-Ordnance
FUS-178	61.22	130.56	0.39	61.15	129.97	0.93	0.080	0.283	0.943	4.96	1.20	1.26	63	-122	-77	357.0	0.971	81-mm Mortar
FUS-179	63.00	127.23	0.16	63.1	127.31	0.11	0.068	0.171	0.972	0.58	0.05	0.24	50	121	-159	960.4	0.957	Frag
FUS-180	60.93	116.11	0.63	60.8	116.24	0.40	0.098	0.512	0.947	3.97	2.37	1.20	23	124	-124	957.8	0.971	81-mm Mortar
FUS-181	67.45	88.93	0.17	67.98	89.09	0.17	0.180	1.137	0.948	18.00	60.23	52.22	13	-37	-45	117.3	0.983	8ventures
FUS-182	70.63	88.05	0.15	70.68	88.08	0.13	0.071	0.193	0.967	7.11	2.96	2.39	-6	-114	22	26947.1	0.949	81-mm Mortar

Target #	Mag Local X (m)	Mag Local Y (m)	Mag Depth (m)	3 β Local X (m)	3 β Local Y (m)	3 β EM Depth (m)	Mag Size (m)	Mag Moment	Fit Quality	β_1	β_2	β_3	Theta	Phi	Psi	χ^2	3 β Coherence	Remediation Results
FUS-183	71.12	85.62	0.37	71.09	85.64	0.36	0.270	10.704	0.846	108.81	11.72	31.51	-4	58	-8	914831.	0.869	Non-Ordnance
FUS-184	75.91	86.17	0.40	75.57	86.52	0.68	0.115	0.890	0.888	70.37	6.42	9.08	70	21	97	117	0.903	Frag
FUS-185	77.42	84.72	0.45	77.59	84.75	0.20	0.121	0.955	0.763	10.73	4.40	8.30	9	80	-101	42512.9	0.945	81-mm Mortar
FUS-186	55.71	132.81	0.48	55.28	132.81	0.39	0.086	0.342	0.917	5.59	1.98	1.45	50	-154	106	1419.2	0.983	81-mm Mortar
FUS-187	45.62	146.87	0.14	45.69	146.82	0.07	0.03	0.163	0.981	5.24	1.04	1.66	13	8	126	275.1	0.922	Non-Ordnance
FUS-188	55.82	143.67	0.77	55.72	143.8	0.47	0.125	1.067	0.951	5.89	4.06	2.07	63	93	-20	999.3	0.978	15-25FragBomb
FUS-189	54.79	150.73	0.42	54.86	150.67	0.34	0.089	0.383	0.977	6.32	2.48	1.51	40	-5	29	7431.4	0.948	81-mm Mortar
FUS-190	50.89	140.98	0.12	50.77	141.02	0.15	0.029	0.014	0.838	1.39	0.37	0.49	6	-2	129	457.5	0.966	Non-Ordnance
FUS-191	46.75	159.70	0.17	46.77	159.72	0.10	0.103	0.593	0.975	0.74	0.13	0.26	17	125	-96	227.4	0.957	Frag
FUS-192	51.15	179.35	0.50	51.31	179.58	0.43	0.077	0.249	0.936	4.91	1.90	2.21	15	38	-171	381.0	0.984	81-mm Mortar
FUS-193	50.45	170.94	0.57	50.45	170.94	0.27			0.981	2.06	0.62	0.81	36	2	22	195.3	0.981	60mmM720
FUS-194	44.21	175.55	0.60	44.13	175.3	0.52	0.074	0.217	0.957	3.96	0.50	1.73	42	-46	172	612.2	0.954	81mm HE M371
FUS-195	45.83	172.30	0.55	45.71	172.28	0.53	0.073	0.214	0.961	3.13	1.47	2.59	-49	149	-170	342.4	0.974	81-mm Mortar
FUS-196	40.04	176.63	0.07	40.01	176.76	0.21	0.036	0.025	0.798	2.61	1.17	1.69	11	35	96	177.9	0.950	Frag
FUS-197	35.78	175.99	0.36	35.87	176.09	0.50	0.061	0.124	0.928	5.57	3.77	2.31	37	-2	-31	604.1	0.975	81-mm Mortar
FUS-198	29.47	176.71	0.33	29.59	176.83	0.37	0.057	0.101	0.958	5.90	2.84	4.43	-26	146	-91	1589.6	0.978	81-mm Mortar
FUS-199	41.30	51.76	0.45	41.38	51.93	0.71	0.085	0.331	0.959	14.02	2.06	5.87	61	-20	166	9362.6	0.871	81-mm Mortar
FUS-200	49.44	48.31	0.17	49.43	48.45	0.23	0.050	0.066	0.939	4.02	0.34	0.66	-2	-78	-116	1604.4	0.931	MK23 SEEDED
FUS-201	90.08	67.30	0.82	90.01	67.52	0.56	0.115	0.828	0.979	5.85	1.61	4.69	6	154	-32	1296.1	0.946	105mm SEEDED